의학박사 학위논문

Production of an anti-ROS1 scFv antibody with enhanced specificity by a point mutation in the HCDR3

HCDR3 의 포인트 돌연변이에 의해 특이성이 증가된 항 ROS1 scFv 항체의 생산

2018 년 02 월

서울대학교 대학원
의과학과 의과학전공
이 화 경

A thesis of the Degree of Doctor of Philosophy

HCDR3 의 포인트 돌연변이에 의해 특이성이 증가된 항 ROS1 scFv 항체의 생산

Production of an anti-ROS1 scFv antibody with enhanced specificity by a point mutation in the HCDR3

February 2018

The Department of Biomedical Sciences,
Seoul National University
College of Medicine
Hwa Kyoung Lee

ABSTRACT

The proto oncogene tyrosine kinase ROS1, which is located at 6p22 on chromosome 6, plays a key role in carcinogenesis through gene rearrangements. Gene rearrangements result in the expression of fusion proteins from partner genes. ROS1 fusion proteins consist of the C-terminal intracellular region of ROS1 and the N-terminal extracellular region of other partners. However, the full-length wild type ROS1 has rarely been reported. The possibility of full-length ROS1 expression has been proposed to be under epigenetic regulation. Here, the 3B20 scFv antibody, which is reactive to the N-terminal region of ROS1, was generated for the detection of full-length ROS1 in cancerous tissues. Unfortunately, in testing the reactivity of the 3B20 scFv antibody, cross-reactivity to the heat shock protein (Hsp) 70 family was also observed during immunoblot and immunoprecipitation analyses. Sequence homology indicated that the Asp, Leu, Gly, and Thr (DLGT) amino acid sequence was shared between ROS1 and Hsp70s. In addition, the epitope was confirmed to harbor this amino acid sequence by alanine scanning mutagenesis of ROS1. To modify the idiotope, which is the unique antigenic determinant of an antibody, random mutations were

introduced into the heavy chain complementary determining region 3 (HCDR3) of the 3B20 scFv antibody. Consequently, a site-direct mutagenesis HCDR3 library was constructed specifically to eradicate cross-reactivity of the 3B20 scFv antibody while maintaining its binding affinity to ROS1. Finally, a new anti-ROS1 clone, 3B20-H1-13 scFv, was successfully generated through point mutation. The 3B20-H1-13 scFv antibody was shown to only react with ROS1 in enzyme-linked immunosorbent assay (ELISA), immunoblot, and immune-precipitation analyses. Immunohistochemistry (IHC) using 3B20-H1-13 scFv showed that ROS1 was absent in non-neoplastic lung tissues, and was overexpressed in a case of lung adenocarcinoma.

Keywords

ROS1, Antibody, Specificity, Mutaion, Epitope

Student number

2009-21902

The results described in this study have been published as *Biochemical and Biophysical Research Communications 2017 Nov 4;493(1):325-331.*

CONTENTS

LIST OF TABLES

LIST OF FIGURES

LIST OF ABBREVIATIONS

ABTS : 2,2’ -azino-bis[3-ethylbenzothiazoline-6-sulphonic acid]

BSA: bovine serum albumin

C_K : kappa light chain constant region

CNG : copy number gain

ELISA : enzyme-linked immunosorbent assay

Fab : fragment antigen binding

Fc : fragment crystallizable

HRP : horseradish peroxidase

HCDR3 : heavy chain complementarity-determining region 3

HA : Hemagglutinin

IHC : immunohistochemistry

KLH : keyhole limpet hemocyanin

mAb : monoclonal antibody

NSCLC : non-small cell lung cancer

OD_{600} : optical density at 600 nm

pIII : protein III

pVIII : protein VIII

PBS : phosphate buffered saline

RTK: receptor tyrosine kinase

scFv : single chain fragment variable

SEC : size exclusion chromatography

TM : transmembrane

INTRODUCTION

1. Lung cancer and its tumor specific factors

Lung cancer is one of the leading causes of cancer-related death worldwide. The primary cause of lung cancer is smoking. However, more than 60% of new cases of lung cancer comprise non-smokers, and 20% women and 8% men diagnosed with lung cancer are non-smokers [1]. Lung cancer is divided into three types, non-small cell lung cancer (NSCLC), small cell lung cancer, and large cell lung carcinoma. NSCLC is the most common type and accounts for 85-90% of lung cancers [2]. Additionally, the survival rate of patients after the diagnosis of NSCLC in stage IV is extremely low (less than 5%). NSCLC can also be divided into three main subtypes. The histological subtypes of NSCLC are adenocarcinoma, squamous cell carcinoma, and large cell carcinoma. In the US, 40% of lung cancer patients suffer from adenocarcinoma [3]. Adeno-carcinoma in NSCLC is known to have several of tumor specific factors, such as KRAS, EGFR, ALK, RET, BRAF, etc [4]. These tumor specific factors have been focused in several studies and cancer therapies. However, these factors must be investigate accurately. For example, copy number variation of EGFR in

Asians has been reported to be more frequent than that of KRAS in non-Asians [5]. Furthermore, in the case of mutated EGFR, gefitinib, which is an EGFR inhibitor, has been used in the treatment of NSCLC patients [6]. Such studies also indicate the importance of investigating tumor specific factors in lung cancer.

2. ROS1 in Lung cancer

Currently, various tumor specific factors expressed in lung cancer have been consistently studying, and one of them is proto-oncogene tyrosine kinase ROS1 (ROS1). ROS1 is the orphan receptor tyrosine kinases (RTKs), and has a large extracellular domain that is composed of fibronectin repeats, a transmembrane domain, and an intracellular kinase domain **(Table 1).** It was first reported in 1986 [7], and was isolated from human glioblastoma cells. ROS1 gene rearrangements was first verified in glioblastoma cell lines [8, 9]. It has been shown that the ROS1 gene on chromosome 6q22 can be rearranged with various partners **(Figure 1).** Therefore, truncated ROS1 protein can be expressed in multiple fusion proteins, where the 3′ region of ROS1 is fused to the 5′ region of v-ros [10], FIG [11], SLC34A2 [12, 13], CD74 [13], EZR [14], LRIG39 [14], TPM3

[14], and SDC4 [15]. In recent studies, ROS1 rearrangements have also been observed in non-small cell lung cancer (NSCLC) [12, 15, 16] and human cholangiocarcinoma [17]. The frequency of ROS1 rearrangement in NSCLC is known to approximately1-2% [12]. Additionally, it is reported that the presence of ROS1 gene copy number gain (CNG) was significantly associated with a higher risk of recurrence of lung cancer, and shorter survival than without ROS1 gene CNG [18]. Furthermore, ROS1 gene CNG is seen as sign an independent poor prognostic factor in NSCLC patients with surgical resection. Therefore, detection of ROS1 is very meaningful to lung cancer patients. ROS1 is known to activate cell signaling associated with proliferation, metastasis, and anti-apoptosis [19];however, its biological functions remain unclear. A lack of adequate information such as unidentified ligand and/ or absence of ROS1 cell lines expressing full-length wild type protein lead to limitations in ROS1 research. Therefore, it is necessary to develop proper antibodies that specifically bind to full-length ROS1, but not to the fusion forms.

3. Overview of antibody phage display technology

When screening an antibody for target molecules, a single chain

fragment variable (scFv) or fragment antigen binding (Fab) are mainly used. Because those molecules size are small than IgG, and it will be simple to handle. After that, a scFv or Fab could be displayed on surfaces of phages, yeasts, bacteria, and ribosomes. Phage display using bacteriophage is a well-known display method; the pIII minor and pVIII major capsid proteins on the phage surface display antibodies, small proteins, or peptides. Phage display technology was first introduced in 1985 by George P. Smith [20], where foreign DNA fragments were inserted into the filamentous phage genome. The phage particle is known to approximately 930 nm in size [21]. The majority of the bacteriophage surface is covered with the 50 amino acid major capsid protein pVIII, at approximately 2,700 copies per phage. The end of the phage particles is composed of minor coat proteins, pIII, pVI, pVII and pIX. All five capsid proteins on the phage particle can be used for phage display. Especially, the pIII and pVIII domains have been frequently used to display peptides and proteins in phage display libraries, as the amino terminal portion of pVIII is present on the outside of phage particles. However, pVIII type phage display libraries have a peptide insertion limit of 6-8 amino acids in length. On the other hand,

the pIII capsid protein consists of three domains, which are N1 or D1, N2 or D2, and CT or D3 domains. The N1 and N2 domains are exposed on the surface of phage particles. Using the pIII phage particle, only approximately 1−2 molecules can be displayed per phage particle. However, it is possible that large insert molecules are well packaged into phage particles, such as scFv, Fab, or other large proteins. Hence, phage display can be used in antibody fragment screening, where it binds to target molecules. Another advantage in using bacteriophage is that it is an economical, high−throughput method, which may arise from its own peculiarities, such as high phage infectivity to *E.coli* cells; infected *E.coli* cells can produce more than a thousand identical phages. In addition, bacteriophages remain stable under various physicochemical stresses, including freeze and thaw cycles [22], as well as exposure to low [23] or high pH [24]. Therefore, bacteriophages can be utilized in various experiments, especially in the phage display system. Similarly, to develop antibody that specifically bind to full−length ROS1, chicken scFvs displayed phage libraries were used in this study.

4. Using bio-panning as antibody screening platform

Bio-panning is an affinity selection method for screening antibodies from phage display libraries. The typical process for bio-panning is as follows **(Figure 2).** First, antibody fragments (scFv or Fab) are displayed on the surface of bacteriophages through antibody fragments-displayed phage library. This library contains a large proportion of antibody displayed on phage. The antibody fragments-displayed phage library is then mixed with target molecules, such as peptides and proteins. At this time, target molecules must be immobilized on solid supports, such as magnetic beads [25], column matrix [26], nitrocellulose [27], polystyrene tubes [28], and 96 well micro-titer polystyrene plates [29]. Non-binding phages are washed out using detergents during the washing steps. Next, the phage bound target molecules are amplified by infecting *E.coli* cells, and this process is repeated. Specific selection processes are then carried out to isolate antibodies against target molecules. Above mentioned bio-panning was used as a well-established screening method to detect the anti-ROS1 scFv antibody. This screening method during natural interactions between antibodies and target molecules is the greatest advantage of phage display

technology. That is also applicable to interaction between scFvs and ROS1 protein, and it is possible to select scFv that specifically binds to ROS1 protein. Consequently, antibodies selected this process will be a valuable tool.

5. Applicability of mass spectrometry analysis to an antibody

Mass spectrometry (MS) analysis is an analytical method that is frequently used to detect intact proteins, peptides, post-translation modifications (PTMs), and metabolites [30]. Moreover, MS analysis could be employed to characterize monoclonal antibody (mAb), including glycosylation, deamidation [31], structure [32], and molecular weight of intact mAbs. Thus, optimized MS analysis has become an essential analytical tool for characterization of mAbs. For example, FDA-approved therapeutic mAbs such as trastuzumab [33], and rituximab [34], were both analyzed and characterized using MS analysis. Furthermore, MS analysis also can be performed with specific antibodies to identify specific protein interaction partners; the protein of interest, along with its partner, is isolated with a specific antibody and then analyzed by MS [35]. Antibody-protein interactions followed by subsequent MS analysis are very

useful for investigation of unknown proteins. For example, dopamine transporter (DAT) interaction proteins, Ca^{2+}/calmodulin-dependent protein kinase II (CaMKII) β, and CaMKII δ were identified from rat striatal synaptosomes by anti-DAT antibodies and LC-MS/MS [36]. Co-immuno-precipitation coupled with MS analysis can identify unknown or multiple protein binding partners. More particularly, liquid chromatography coupled with tandem mass spectrometry (LC-MS/MS) data is generally quantified using the spectral counting [37]. Spectral counting is based on the observation of identified number of spectra, and more abundant peptides will be selected for fragmentation [38]. And then, protein can be predicted from the collected abundant peptides. The anti-ROS1 scFv antibody developed through bio-panning was observed non-specific binding to some protein, not ROS1. Above mentioned method was actually used to identify non-specific binders of anti-ROS1 scFv antibody. The protein was identified using spectral counting, and the information of that was very helpful in the characterization and modification of the developed antibody.

6. Specificity of an antibody

Antibodies development by several methods, including bio-panning are widely used for antigen detection in various assays, such as enzyme immunoassays, radioimmunoassays, and fluorescence immunoassays. For these assays, antibodies can be labeled with diverse compounds including enzymes, radioisotopes, and fluorochromes. Also, various antibody technologies for simultaneous detection of multiple antigens are under active development. In brief, numerous mAb are being developed each year for specific assays; however, many of these mAbs have demonstrated cross-reactivity, variability in quality, and have been used in wrong applications [39]. The Human Atlas is an open database that stores protein profiles based on thousands of antibodies against cancer, normal tissues, and cell lines. This database is heavily antibody dependent; however, it has been reported that more than 50% of commercially available antibodies have poor specificity, or do not work at all [40]. Furthermore, most commercially available antibodies demonstrate cross-reactivity. During the establishment of the size exclusion chromatography-microsphere based affinity proteomics (SEC-MAP) method, more than 1,500 commercially

available antibodies were tested by size exclusion chromatography (SEC). Results indicated that most commercially available antibodies bind to more than one target [41]. That is very undesirable, because antibody are considered an reaction of one antigen. Eventually, it is related to antibody's specificity. Antibody specificity refers to the ability of antibody which reacts with a one target. The key advantage of using mAbs in therapy, agonist, antagonist, and ELISA kit is also its specificity. Occasionally, antibody specificity is regarded as a magic bullet. That is why antibody specificity should be investigated and enhanced after or during antibody development.

PURPOSE OF THE STUDY

The proto oncogene tyrosine kinase ROS1 is an orphan receptor whose ligand has not yet been identified. Due to the unidentified ligand, the functions of wild type ROS1 are almost unknown. The ROS1 gene is unique in that it frequently undergoes gene rearrangements. Therefore, the ROS1 protein is mainly expressed in fusion proteins with N-terminal partners including FIG, CD74, and SLC34A2. The function of ROS1 has been studied from these fusion ROS1 proteins. To investigate the expression of wild type ROS1, an antibody that binds to the N-terminal of ROS1 is required. Furthermore, N-terminal binding of the ROS1 antibody could enable it to act as an agonist or antagonist. The writer of this thesis developed an anti-ROS1 scFv antibody, which was able to bind to the N-terminus of ROS1. The anti-ROS1 scFv antibody epitope was well-defined by alanine scanning mutagenesis, and showed high reactivity against ROS1. However, cross-reactivity to Hsp70s was observed in anti-ROS1 scFv antibody as well. To eradicate cross-reactivity, a point mutation was introduced into the HCDR3 of the antibody. The purpose of this study was to develop an anti-ROS1 scFv antibody, and to enhance its specificity through point mutations

in the HCDR3. The modified anti-ROS1 scFv antibody can be useful in investigating the full-length ROS1, and can reveal uncovered biological function of the full-length ROS1.

MATERIALS AND METHODS

1. Development of anti-ROS1 scFv antibody, 3B20

1-1. Immunization of ROS1 peptide

Three White Leghorn chickens were immunized four times with the synthetic peptide (TNLGQQLDLGTPHNLSEPGGGC) of ROS1 (NCBI Reference Sequence: NP_002935.2) conjugated with keyhole limpet hemocyanin (KLH) (Peptron; Daejun, Korea). Boost immunizations were performed at three times in chickens with 2-3 week intervals. (Table 2) The antibody titer was determined by enzyme linked immunosorbent assay (ELISA) against ROS1 peptide and recombinant proteins.

1-2. Enzyme-linked immunosorbent assay with immunized chicken serum

ELISA using immunized chicken serum was performed against ROS1 N-terminus peptide and recombinant ROS1 proteins. Ninety-six well microtiter plates (Corning Costar Corp., Cambridge, MA, USA) were coated with 100 ng of ROS1 N-terminus (39~56) peptide conjugated with bovine serum albumin (BSA), recombinant ROS1 (37-290 amino acids)-hFc

and C_K fusion protein per well for overnight at 4℃. After day, the wells were blocked with 100 μL of 3% BSA in PBS. Chicken sera of first injection, 1st boosting, and 2nd boosting were diluted 1/500, 1/1000, 1/2000, 1/4000, and 1/8000 in 3% BSA in PBS. Each diluted chicken sera added to well and incubated for 2 h at 37℃. After washing with 0.05% Tween 20 in PBS (PBST) three times, plates were incubated with HRP conjugated anti-chicken IgY antibody (Merck, Kenilworth, NJ, USA). Washing steps were repeated three times. 2,2' -azino-bis(3-ethylbenzothiazoline-6-sulphonic acid) (ABTS, Amresco, Solon, OH, USA) in 0.05 M Citric acid buffer (pH 4.0) and 1.0% H_2O_2 were added to each well. Optical density was measured at 405 nm with microplate photometer (Labsystems Multiskan Ascent microplate reader, Thermo Fisher Scientific, Rockford, IL, USA)

1-3. Immunoblot assay with immunized chicken serum

HEK 293T cells transfected with Lentiviral vector encoding human ROS1 and GFP cell lysates were separated on 4-12% Bis-Tris SDS-polyacrylamide gel (Thermo Fisher Scientific) and transferred to a nitrocellulose membrane (Whatman, Maidstone, Kent, UK). The membrane was blocked with 5% skim

milk in Tris-buffered saline (TBS) containing 0.2% tween-20 at room temperature for 1 h and then incubated overnight with the 1^{st} boosting, and 2^{nd} boosting sera. The serum was diluted 1/2000 in blocking buffer. The membrane was washed five times with 0.2% tween-20 in TBS. HRP-conjugated anti-chicken IgY antibody (Merck) were used as secondary antibodies diluted 1:5000 in blocking buffer for 1 h at room temperature. The blots were visualized using the enhanced chemiluminescence system (Thermo Fisher Scientific), according to the manufacturer's instructions.

1-4. Extraction of total RNAs and synthesis of cDNAs

Total RNAs was isolated from the harvested spleen, bone marrow, and bursa of Fabricius using the TRI Reagent® (Thermo Fisher Scientific) according to the manufacturer's instruction. First-strand cDNAs were synthesized using the synthesized First-strand cDNA kit (Thermo Fisher Scientific) and first round of PCR was performed using Expand High Fidelity PCR system (Roche, Basel, Switzerland). For chicken scFv libraries, one primer combination was used for each of V_λ and V_H amplification (Table 3, Figure 3).

1-5. Construction of chicken scFv phage display libraries

Three phage displayed chicken single-chain variable fragments (scFv) libraries were constructed using the pComb3XSS phagemid vector. In each reaction, one μL of cDNA was mixed with 80 pmol of each primer, 10 μL of 10 X reaction buffer, 8 μL of 2.5 mM dNTPs, 1 μL of Taq DNA polymerase and water to a final volume of 100 μL. The PCR reactions were carried out under the following condition: 30 cycles of 15 s at 94℃, 30 s at 56℃, and 90 s at 72℃, followed by a final extension for 10 min at 72℃. Amplified fragments with length of approximately 350 base pairs were loaded and run on a 1.5% agarose gel, and purified with Gel Extraction Kit (Qiagen, Netherlands, Hilden, Germany). The primer sets for this were as described above. (Table 3) In the second round of PCR, the first round V_L products and V_H products were randomly joined by overlap extension PCR. Overlap Extension Primers sets were as described above. (Table 3) Each PCR reaction was performed in a 100 μL mixture composed of 100 ng of purified V_L product and V_H product, 60 pmol of each primer, 10 μL of 10 X reaction buffer, 8 μL of 2.5 mM dNTPs and 1 μL of Taq DNA polymerase. The PCR reactions were carried out under the following condition: 20

cycles of 15 s at 94℃, 30 s at 56℃, and 2 min at 72℃, followed by a final extension for 10 min at 72℃. About 700 base pairs sized scFv fragments were purified with Gel Extraction Kit (Qiagen). The scFv fragments and pComb3XSS phagemid vectors were digested with *Sfi* I restriction enzyme (Roche) by incubating for 8 h at 50℃. Seven hundred ng of *Sfi* I-digested scFv was ligated with 1,400 ng of pComb3XSS phagemid vector using T4 DNA ligase (Thermo Fisher Scientific) by incubating the reaction mixture for 16 h at 16℃, followed by ethanol precipitation.

1-6. Amplification of phage display libraries

Ligated library DNA was transformed into 300 μL of electrocompetent *E. coli* ER2738 (New England Biolabs, Beverly, MA, USA) by electroporation with a 0.2 cm cuvette and Gene Pulser (Bio-Rad Laboratories, Hercules, CA, USA) at a condition of 2.5 kV, 25 μF and 200 Ω. The cells were resuspended with 3 mL of Super Broth (SB) medium and incubated for 1 h at 37℃ while shaking at 250 rpm. 10 mL of SB medium and 3 μL of 100 mg/mL carbenicillin were added to the culture. The library size was determined by plating 0.1, 1 and 10 μL of the culture on

Luria Broth (LB) plate containing 50 μg/mL of carbenicillin. After one hour of incubation, 4.5 μL of 100 mg/mL carbenicillin was added to the culture and incubate for an additional hour. The culture was added to 10 mL of VCSM13 helper phage (> 10^{11} cfu/mL, New England Biolabs), 173 mL of SB medium and 92.5 μL of 100 mg/mL carbenicillin and incubated for 2 h at 37℃ while shaking at 250 rpm. Kanamycin (280 μL) was added to the culture, and the culture was shaken overnight at 250 rpm and 37℃. The next day, the culture was centrifuged at 3,000 x *g* for 15 min. The bacterial pellets were saved for phagemid DNAs preparation and the supernatant was transferred to clean centrifuge bottle. Eight grams of polyethylene glycol-8000 (PEG-8000) and 6 g of NaCl (Merck) were added, and the supernatant was stored on ice for 30 min. The supernatant was spun at 15,000 x *g* for 15 min at 4℃. The phage pellets were resuspended in Tris-buffered saline (TBS) containing 1% BSA.

1-7. Preparation of bacteriophages

A single plaque was selected from the titration plate and used to infect 10 mL of *E. coli* ER2738 cells in the exponential growth phase, optical density at 600 nm (OD_{600}) = 0.8. The cells were

allowed to grow with shaking at 250 rpm for 2 h at 37 ℃. The culture was added to 500 mL of SB containing kanamycin (70 μg/mL) and incubated overnight at 37 ℃ with shaking at 250 rpm. After centrifugation at 3,000 x *g* for 15 min, the culture was transferred to 500 mL tubes and incubated in a water bath at 70 ℃ for 20 min. The culture was then centrifuged at 3,000 x *g* for 15 min. Finally, the supernatants transferred to new tubes and stored at 4 ℃ until used.

1-8. Preparation of electro-competent cells

A single colony of *E. coli* ER2738 was inoculated to 10 mL of prewarmed SB medium and incubated overnight at 37℃. The next day, 2.5 mL of the culture was transferred into 500 mL SB medium containing 10 mL of 20% (w/v) glucose and 5 mL of 1 M $MgCl_2$ and shook at 250 rpm and 37℃ until the OD_{600} reaches 0.8. The culture was poured into prechilled 500 mL of centrifuge bottle and incubated 15 min on ice. The culture was separated into supernatant and pellets by centrifugation at 3,000 x *g* for 20 min at 4℃. The supernatant was discarded and the pellets were resuspended in 250 mL of prechilled 10% (w/v) glycerol solution. The resuspension was spun as before. After three times of

pellets washing, the supernatant was discarded and the pellets were resuspended in 3 mL of 10% glycerol solution, and aliquoted at small volumes stored at −80℃.

1−9. Bio−panning

Two point five μg of ROS1 N−terminus (39~56) peptide conjugated with KLH and recombinant ROS1 (37−290 amino acids)−hFc were coated to 5 x 10^6 dynabeads (M270− Epoxy, Thermo Fisher Scientific) at room temperature for 18 h. The beads were washed with 500 μL of 3% BSA in PBS at 5 times and blocked with 3% BSA in PBS at room temperature for 1 h. After washing of ROS1 peptide and protein coated beads with 0.5% PBST briefly, beads were incubated with phage−displayed scFvs at room temperature for 2 h. The beads were washed with 500 μL of 0.5% PBST for removing unbound phage. The number of washing steps was increased from once in first round to 5 times in fifth round of panning. Bound phages were eluted using 60 μL of 0.1 M Glycine−HCl (pH 2.2) at twice and neutralized by 6 μL of 2 M Tris−HCl (pH 9.1). Eluted phages were used to infect 2 mL of *E. coli* ER2738 and the phagemid was rescued with 5 mL of VCSM13 helper phage for overnight amplification. The input

and output phage titer were determined by plating the phage infected bacterial culture on LB plate containing 50 μg/mL of carbenicillin. Next day, the phage was precipitated by adding PEG and NaCl as described above.

1-10. Individual phage enzyme-linked immunosorbent assay

ELISA using phages displaying scFvs was performed against ROS1 peptide and protein to analyze the selected clones from bio-panning. Ninety-six well microtiter plates (Corning Costar Corp.) were coated with 100 ng of ROS1 N-terminus (39~56) peptide conjugated with BSA, recombinant ROS1 (37-290 amino acids)-hFc and mouse anti-Hemagglutinin (HA) antibody per well for overnight at 4℃. After day, the wells were blocked with 100 μL of 3% BSA in PBS. Each phage culture was mixed with an equal volume of 6% BSA in PBS and incubated for 2 h at 37℃. After washing with 0.05% PBST three times, plates were incubated with HRP conjugated anti-M13 antibody (GE Healthcare Life Sciences, Piscataway, NJ, USA). Washing steps were repeated three times. ABTS solution in 0.05 M Citric acid buffer (pH 4.0) and 1.0% H_2O_2 were added to each well. Optical

density was measured at 405 nm with microplate photometer (Labsystems Multiskan Ascent microplate reader, Thermo Fisher Scientific)

2. Overexpression and purification of anti-ROS1 scFv antibody

2-1. Sub-cloning of anti-ROS1 scFv antibody into Fc and C_K vector

The vector carries an expression cassette composed of the leader sequence of the human Ig κ-chain, two *Sfi* I sites for insertion of the antibody gene of interest, the hinge region of human IgG_1,and the CH_2–CH_3 domains of rabbit IgG. For C_K fusion, gene encoding human IgG_1 hinge and human C_K was inserted into pCEP4 vector. Then the gene encoding anti-ROS1 scFv antibody derived bio-panning was sub-cloned in the 5' end of Fc region by two *Sfi* I restriction sites, followed by ligation using T4 DNA ligase (Thermo Fisher Scientific), as described previously.

2-2. Transient transfection and affinity chromatography purification

DNA for transfection was prepared using PureLink HiPure Plasmid Maxi-prep kit (Thermo Fisher Scientific), according to the manufacturer's instructions. Transfection was performed into HEK 293F cells (1.0 x 10^6 cells/mL, Thermo Fisher Scientific) using polyethylenimine (PEI, Polysciences, Warrington, PA, USA). Two point five μg of mammalian expression vector per mL of culture volume and 5 μg of polyethyleneimine/mL were mixed in 150 mM NaCl (1/10 volume of total), and let stand at room temperature for 15 min. The mixture was added to the HEK 293F cells (2 x 10^6 cells/mL, Thermo Fisher Scientific) and cultured for 6 days under the following condition : FreeStyle™ 293 Expression medium (Thermo Fisher Scientific) containing 100 U/mL penicillin (Thermo Fisher Scientific) and 100 U/mL streptomycin (Thermo Fisher Scientific), 37℃, 7% CO_2, 135 rpm on an orbital shaker. Each protein was purified by protein A agarose beads (Repligen, Waltham, MA, USA) or the KappaSelect resin (GE Healthcare, Piscataway, NJ, USA), according to the manufacturer's instructions.

3. Construction and production of lentivirus

To generate the pLenti6-human ROS1-DEST construct, pENTR223.1-human ROS1 (Open Biosystems, Huntsville, AL, USA) was transferred into pLenti6/V5-DEST (Thermo Fisher Scientific) through Gateway recombination cloning technology using Gateway LR ClonaseTM (Thermo Fisher Scientific) according to manufacturer's instructions. The pLenti6-human ROS1-DEST construct used for lentiviral production was confirmed by sequencing through Primer Walking system (Macrogen, Seoul, South Korea). To produce negative control virus to be used, green fluorescent protein (GFP) was also cloned into the same lentiviral vector.

Lentivirus was produced by transient transfection of HEK 293T cells. pLenti6-GFP-DEST or pLenti6-human ROS1-DEST lentiviral construct was co-transfected with vesicular stomatitis virus glycoprotein (VSV-G) plasmid DNA and delta 8.9 (Gag-pol) plasmid DNA for viral packaging into HEK 293T cells using lipofectamine 2000 (Thermo Fisher Scientific) reagent according to manufacturer's instructions. The medium was replaced with fresh medium at 6 h post-transfection. Supernatant of transfected cells were harvested at 48 h after transfection and

filtered by 0.45 ㎛ membrane (Pall Corporation, Washington, NY, USA). Viral particles were concentrated and purified using a Lenti-X concentrator (Clontech Lab, Mountain View, CA, USA) according to manufacturer's instructions.

4. Transduction and establishment of ROS1 stable cell line

To generate full-length recombinant ROS1 overexpressing cell lines, HEK 293T cell were infected with pLenti6-GFP-DEST or pLenti6-human ROS1-DEST expressing lentiviruses in the presence of 6 ㎍/mL polybrene. The transduction efficiency was determined by parallel control experiments. Green fluorescence of the cells transduced with GFP lentivirus generated at the same time with ROS1 lentivirus was observed after 72 h. Antibiotic selection using 10 μg/mL of blasticidin (Thermo Fisher Scientific) was performed on the virally infected cells for 7 days. The blasticidin resistant lentivirus infected cells were selected and stable cell lines were established. mRNA and protein expression level of human ROS1 were verified by reverse transcription polymerase chain reaction (RT-PCR) and immunoblots, respectively (data not shown).

5. Cell culture

HEK 293T lentiviral transfected ROS1 and GFP cells were cultured in Dulbecco's modified Eagle's medium (DMEM; Welgene, Seoul, Korea) supplemented with 10% heat inactivated FBS (GIBCO, Grand Island, NY, USA), 100 U/mL penicillin and 100 mg/mL streptomycin, 2 mM L-Glutamine (GIBCO) in a humidified 5% CO_2 atmosphere at 37℃.

6. Immunoblots

Cell lysates were separated on 4-12% Bis-Tris SDS-PAGE gel (Thermo Fisher Scientific) and transferred to a nitrocellulose membrane (Whatman). The membrane was blocked with 5% skim milk in Tris-buffered saline (TBS) containing 0.2% tween-20 at room temperature for 1 h and then incubated overnight with 3B20 scFv-rabbit Fc (rFc) fusion protein (200 ng/mL), 3B20-H1-13 scFv-rFc fusion protein (1 μg/mL), anti-ROS1 antibodies (ab5512; 1:1000 dilution; Abcam), (3266; 1:1000 dilution; Cell Signaling Technology) or anti-tubulin antibody (1:5000 dilution; Santa Cruz, Dallas, Texas, USA). The blots were washed five times with 0.2% tween-20 in TBS. HRP-conjugated anti-rabbit IgG (Fc-specific) antibody (Abcam) and

anti-mouse IgG antibody (Pierce Chemical Co., Rockford, IL, USA) were used as secondary antibodies diluted 1:5000 in blocking buffer for 1 h at room temperature. The blots were visualized using the enhanced chemiluminescence system (Thermo Fisher Scientific), according to the manufacturer's instructions.

7. Immunoprecipitation and pull-down assay

Lentiviral transduced HEK 293T cells which overexpress either ROS1 or GFP were lysed in cold lysis buffer [1% Triton X-100, 150 mM NaCl, and 50 mM Tris. (pH8.0)] containing 1 mM PMSF (Merck), protease inhibitor cocktail (Roche), Phosphatase inhibition cocktail (Roche). Total lysates were incubated with 3B20 scFv and 3B20-H1-13 scFv fused to rFc fusion protein (5 μg/mL) at 4℃ for overnight with rotation. The 20 μL of protein A agarose beads (Repligen) were washed three times with PBS and once with lysis buffer and added to lysates, followed by incubation at 4℃ for 4 h. After beads were washed three times with PBS, proteins bound beads were eluted by boiling in NuPAGE LDS Sample Buffer (Thermo Fisher Scientific) and subjected to immunoblots analysis, as described above. For

pull-down assay, eluted proteins were separated by SDS-PAGE gel and stained using Coomassie Blue R250 (Merck), according to the manufacturer's instructions.

8. Epitope mapping of anti-ROS1 scFv antibody, 3B20

8-1. Preparation of alanine substituted proteins

For epitope mapping of 3B20 scFv, alanine scanning mutagenesis assay was performed. Recombinant ROS1 (37-290 amino acid) protein was used as the template and amino acid residues from Gly_{42} through Ser_{54} of ROS1 were replaced with alanine by PCR experiment. Total of 13 residues were replaced with alanine one at a time; primer sequences were as follows: Forward: 5'-GGCCCAGGCGGCCTGTGTAACTAATCTG[GGC/CAG/CAG/CT T/GAC/CTT/GGC/ACA/CCA/CAT/AAT/CTG/AGT]GAACCGTG T-3', Reverse: 5'-GGCCGGCCTGGCCTTCCTCTTGTTGAA CTGCTGA-3' (each amino acid in the slash was replace with alanine). PCR was performed according to the initial denaturation at 94℃ for 5 min, 25 cycles of denaturation at 94℃ for 30 s, annealing at 55℃ for 30 s, extension at 72℃ for 1 min and final extension 72℃ for 10 min. PCR product was subjected to 1% agarose gel electrophoresis and purified using QIAquick Gel

Extraction Kit (Qiagen) according to the manufacturer's instructions. Purified gene fused to modified human IgG1 Fc was sub-cloned into pCEP4 mammalian expression vector, as described above.

8-2. ELISA using mutagenesis of the 3B20 scFv

For alanine scanning mutagenesis of the 3B20 scFv, 96 well microtiter plates (Corning Costar Corp.) were coated with 100 ng of the 3B20 scFv-C_K fusion protein, BSA, or irrelevant scFv-C_K fusion protein overnight at 4℃ and blocked with 100 ㎕ of 3% BSA in PBS for 1 h. The plates were incubated with alanine substituted ROS1-hFc fusion proteins (each amino acid residue from Gly_{42} to Ser_{54} were replaced with alanine) and original (not replaced with alanine). After three times washing with 150 ㎕ of 0.05% PBST, plates were incubated with HRP-conjugated Rabbit anti-Human IgG Fc antibody (1:5000 dilution; Thermo Fisher Scientific) for 1 h at 37℃. The plates were washed with 150 ㎕ of 0.05% PBST and binding of the alanine substituted ROS1 protein were determined by adding ABTS solution, as described above. All experiments were performed in triplicates.

9. Site-directed HCDR3 mutagenesis libraries of the 3B20 scFv

To generate HCDR3 site-directed mutagenesis libraries, 3B20 scFv was used as the template for library construction using degenerate codon NNK (N = A, T, G and C and K = G and T). First fragment was amplified using forward primer 5'-CTGGCTGGTTTCGCTACCGTGGCC-3' and reverse primer 5'-TCTGGTGCAGTAGTAGGTGGC-3' and second fragment was amplified using forward primer 5'-GCCACCTACTACTGCACCAGA[GGT/GGT/GGT/GGT/AAC/ATC/GAC/GCA]TGGGGCCAC-3' and reverse primer 5'-CGGGTATGCGCCATGGTGATGGTG)-3' by PCR experiments, as described above (Each amino acid in the slash was replaced with NNK,). Subsequently, these PCR fragments were purified, followed by overlap extension PCR. One-hundred ng of PCR products were mixed in equal ratios to generate the overlap extension product as described above. The scFv genes, purified overlap extension PCR products, was ligated into the pComb3XSS phagemid vector followed by phage ELISA as described above.

10. Enzyme-linked immunosorbent assay (ELISA)

Ninety-six well microtiter plates (Corning Costar Corp.) were coated overnight at 4℃ with 100 ng of recombinant ROS1 (37-290 amino acids)-C_K fusion protein, the irrelevant protein-C_K fusion molecule, the synthetic peptide (TNLGQQLDLGTPHNLSE PGGGC) or GRP75 (Enzo Life Sciences, Farmingdale, NY, USA) dissolved in coating buffer (0.1 M sodium bicarbonate, pH 8.6). Plates were blocked with 100 ㎕ of 3% BSA in PBS for 1 h at 37℃. Anti-ROS1 scFv antibodies, 3B20 scFv and 3B20-H1-13 scFv fused to rFc were added to wells in a dose dependent manner in blocking buffer and incubated at 37℃ for 2 h. After three times washing with 0.05% PBST, plates were incubated with 50 ㎕ of HRP-conjugated goat anti-rabbit IgG (Fc-specific) antibody (1:5000 dilution in blocking buffer; Abcam, Cambridge science park, Cambridge, UK) for 1 h at 37℃. After three times washing, ABTS solution was added to each wells, and optical density was measured at 405 nm (Labsystems Multiskan Ascent microplate reader, Thermo Fisher Scientific).

11. Mass spectrometry analysis

Protein bands about 70 kDa and 260 kDa in the SDS-PAGE gel

were excised, and subjected to in-gel tryptic digestion as described previously. Excised protein bands were destained, reduced with 20 mM DTT, and then alkylated with 55 mM iodoacetamide. After dehydration with acetonitrile (ACN), the proteins were digested with 12.5 ng/μL modified trypsin (Promega, Madison, WI, USA) in 50 mM ammonium bicarbonate overnight at 37 ° C. Peptides were extracted from the gel slices with 50% (v/v) ACN in 0.1% (v/v) formic acid (FA). The eluates were dried under a Centrivap concentrator (Labconco, Kansas City, MO, USA). Extracted peptide samples were suspended in 0.1% formic acid in water, loaded onto an EASY-Spray C18 column (75 μm×50 cm, 2 μm) and separated with a 2-35% gradient of 0.1% formic acid in acetonitrile for 65 min at a flow rate of 300 nL/min. MS spectra were recorded on a Q-Exactive hybrid quadrupole-Orbitrap mass spectrometer (Thermo Fisher Scientific) interfaced with a nano-ultra-HPLC system (Easy-nLC1000; Thermo Fisher Scientific). Collected MS/MS raw files were converted to mzXML files using the Trans-Proteomic Pipeline (version 4.4) and analyzed using the Sequest (version 27) algorithm in the SORCERER (Sage-N Research, Milpitas, CA, USA) platform. The search was performed using the IPI human

database (version 3.83, 186578 entries). Full tryptic specificity and up to two missed cleavage sites were allowed. Mass tolerances for precursor ions and fragment ions were set to 10 ppm and 1 Da, respectively. Fixed modification for carbamidomethyl-cysteine and variable modifications for methionine oxidation were used. All proteins with a ProteinProphet probability of ≥ 99% with minimum three peptides and a PeptideProphet probability of ≥ 95% were identified using Scaffold (version 4.3.2; Proteome Software, Portland, OR, USA).

12. Immunohistochemistry

Representative paraffin blocks were cut into 4-μm-thick sections and examined for IHC using an automated immunostainer (Ventana BenchMark XT, Tuscan, AZ, USA). Heat-induced epitope retrieval with Ventana CC1 mild reagent was applied and endogenous peroxidase was blocked by 3% H_2O_2 for 10 min. The slides were incubated with 3B20 scFv-rFc and 3B20-H1-13-rFc (300 μg/mL stock; 1:100 dilution) fusion protein for an hour. Visualization was done with diaminobenzidine tetrachloride.

RESULTS

1. ELISA and immunoblot analysis with serum for confirmation of anti-ROS1 antibodies

To generate an anti-ROS1 antibody, chicken serum ELISA was performed using ROS1 (37-290)-hFc fusion proteins, ROS1 (37-290)-C_K fusion proteins and ROS1 synthetic peptides (TNLGQQLDLGTPHNLSEPGGGC, amino acid 39-56 of ROS1) were conjugated with KLH **(Figure 4)**. Following immunization of chickens with the peptide (39-56)-conjugated to KLH at the N-terminus, immunoblot assay was performed using chicken serum **(Figure 5)**.

2. Generation of the anti-ROS1 scFv libraries and screening for specific binding to the N-terminus of ROS1

Using total RNAs isolated from the spleen, the bursa of Fabricius, and the bone marrow of immunized chicken, chicken scFv libraries with complexities of 8.7×10^9, 5.9×10^9, and 7.2×10^9 was generated. The quality of the RNA, PCR products, and test ligation were assessed by electrophoresis with agarose gel and electroporation with test ligated samples **(Figure 6)**. After five

rounds of bio-panning (Table 4), phage enzyme-linked immunosorbent assay (ELISA) was performed to isolate positive clones (Figure 7). Selected 3B20 scFv phage clones showed binding reactivity against both the recombinant N-terminus ROS1 (amino acid 37-290) C_K fusion protein and the ROS1 synthetic peptide (Figure 8A). Subsequently, the 3B20 scFv gene was sub-cloned into modified pCEP4 expression vectors containing the Fc region of rabbit IgG (scFv-rFc), which were transfected into HEK 293F cells using the PEI reagent. After five days, affinity chromatography was performed using protein A agarose beads in order to purify recombinant 3B20 scFv-rFc fusion proteins from the cultured supernatant. Binding reactivity of purified 3B20 scFv-rFc fusion proteins to recombinant ROS1 proteins and peptides was evaluated by ELISA (Figure 8B). Pull-down assays were performed using HEK 293T cells lysates transfected with lentiviral vectors encoding the human ROS1 (full-length). These lysates were incubated with 3B20 scFv-rFc fusion proteins and protein A agarose beads. After protein A agarose beads were washed, proteins bound to beads were eluted in the SDS-PAGE sample buffer. The eluted proteins were subjected to SDS-PAGE, and were identified using mouse

anti-ROS1 (69D6) mAbs (#3266; Cell signaling, Danvers, MA, USA). ROS1, which corresponded to a band with a molecular weight of 260 kDa, was clearly detected (Figure 9B). However, in the case of direct immunoblot assays using the 3B20 scFv, multiple bands including the recombinant ROS1 protein were detected from transfected cell lysates (Figure 9A).

3. Identification of the putative antibody epitope from mass spectrometry and protein homology analysis

To investigate the epitope of 3B20 scFv, pull-down assay was performed using 3B20 scFv-rFc fusion proteins from HEK 293T cells transfected with lentiviral vectors encoding the human ROS1 (full-length) and GFP (control) genes. Proteins bound to the 3B20 scFv protein were separated by SDS-PAGE. Following electrophoresis, the gel was stained with Coomassie Blue R250 (Figure 10). Bands corresponding to 70 and 260 kDa were excised from the gel, and were analyzed by mass spectrometry (Figure 11). The top 10% of the spectral numbers were displayed in descending order, and as expected, the majority of ROS1 (Accession number: IPI0028965) proteins were detected at approximately 260 kDa (Figure 11). Due to non-specific

immunoblots bands at approximately 70 kDa, I investigated this region in more detail. Interestingly, 70 kDa heat shock proteins (Hsp70s) were also abundantly expressed in both ROS-transfected and control gels. To determine the cause of unspecific binding to Hsp70s, the Hsp70s sequence was compared with that of the ROS1 protein using BLAST at the NCBI database. I found that both Hsp70s and ROS1 have the same amino acid sequence (Asp, Leu, Gly, and Tyr) in the exact same order. These sequences were identical to the D_{59} L_{60} G_{61} T_{62} sequence of 75 kDa glucose regulated protein (GRP75), and can also be found in other members of Hsp70s. Therefore, I hypothesized that the epitope of the 3B20 scFv should be D_{46} L_{47} G_{48} T_{49} in ROS1.

4. Epitope mapping of the 3B20 scFv via alanine scanning mutagenesis assay

To further confirm the epitope of the 3B20 scFv, alanine scanning mutagenesis assay was performed using phage form and recombinant ROS1 proteins (corresponding to 37-290 amino acids of ROS1). Each amino acid from Gly_{42} to Ser_{54} in the ROS1 protein was substituted by alanine (Ala) **(Figure 12)**. The 3B20

scFv−C_K fusion protein (100 ng) or an irrelevant scFv−C_K fusion protein was individually coated onto 96 well microtiter plates. After blocking the plate with BSA, alanine substituted mutant phage with different mutagenesis sites were added into each well. Binding reactivity of the alanine substituted ROS1 mutant phages to the 3B20 scFv was determined using HRP−conjugated M13 antibodies **(Figure 13A)**. Because pComb3XSS phagemid vector has a HA tag at the C terminus of the scFv, the anti−HA signal of phages was also determined for phage amplification. (Data not shown). The absorbance of phage amplification is set to 1, then the relative absorbance of ROS1 mutant binding is measured. The recombinant ROS1−hFc fusion protein (100 ng) substituted with alanine was also similarly coated. Following blocking, the 3B20 scFv−C_K fusion protein was added. The amount of bound 3B20 scFv was determined using HRP−conjugated anti−C_K antibodies and the ABTS solution **(Figure 13B)**. The amount of coated ROS1−hFc fusion protein was determined using HRP−conjugated anti−hFc antibodies. (Data not shown) The absorbance of coated protein is set to 2, then the relative absorbance of the ELISA signal of 3B20 scFv binding is measured. (Data not shown). The three alanine substituted ROS1

mutants, $Gly_{42}Ala$, $Gln_{43}Ala$, and $Gln_{44}Ala$ showed slightly higher binding reactivity to the 3B20 scFv as compared with that of the recombinant ROS1 protein. On the contrary, $Leu_{45}Ala$, $Leu_{47}Ala$, and $Gly_{48}Ala$ mutants did not demonstrate binding reactivity to the 3B20 scFv **(Figure 14A)**. The rest of the mutants showed similar or slightly lower binding reactivity to the 3B20 scFv. No background signal was detected in the blocking-buffer-only sample **(Figure 14B)** or the irrelevant scFv-C_K fusion protein sample **(Figure 14C)**. I concluded that Leu_{45}, Leu_{47}, and Gly_{48} of ROS1 play critical roles in binding specificity of the 3B20 scFv.

5. Screening of modified 3B20 scFv with altered specificity from the HCDR3 site-directed mutagenesis libraries

It was found that the 3B20 scFv demonstrate multi-reactivity via immunoblot and immunoprecipitation analyses. This was confirmed by mass spectroscopy, whereby 3B20 scFv was found to bind to Hsp70s. Reactivity of the 3B20 scFv to ROS1 and Hsp70 was assessed by ELISA **(Figure 15)**. To eliminate non-specific binding of the 3B20 scFv, I constructed HCDR3 site-directed mutagenesis libraries through PCR. The 3B20 scFv consists of eight amino acids in the HCDR3, and each amino acid

was substituted with NNK degenerate codons (Figure 16). From the eight HCDR3 site-directed mutagenesis libraries constructed, 48 clones were selected, followed by amplification to phage. I then performed phage ELISA to evaluate their binding reactivity against both recombinant ROS1 and GRP75 (Figure 17). The anti-HA signal of phages was also determined for phage amplification, and it was confirmed that all phage signal was evenly amplified. (Data not shown). Relative absorbance after subtraction of the reduced blocking only was measured. Interestingly, some of the amino acid changes in HCDR3 had significant effects on antibody binding reactivity. Approximately 60% of clones from libraries generated by NNK randomization at the 2^{nd}, 3^{rd}, or 4^{th} amino acid position in the HCDR3 have lost their binding reactivity to recombinant ROS1, GRP75, or both ROS1 and GRP75. Approximately 30% of the clones from the 1^{st} position randomized library lost their binding reactivity. On the other hand, 80-90% of the clones from 5^{th}, 6^{th}, 7^{th}, and 8^{th} position randomized libraries still maintained binding reactivity to both the recombinant ROS1 and GRP75. One candidate clone was isolated from the 1^{st} position randomized library that exhibited binding reactivity to ROS1, but not to GRP75. Selected

candidate clones were sub-cloned into pCEP4-rFc vectors, and were transfected into HEK 293F cells. Following affinity purification using protein A agarose beads, the eluted protein was subjected to SDS-PAGE, and was stained by Coomassie Blue R250 (Figure 18). Reactivity of selected candidate clones to ROS1 and GRP75 was also determined by ELISA using the recombinant ROS1 protein (Figure 19) and the ROS1 peptide (Figure 20). Immunoblot was also performed to test binding of candidate clones to recombinant ROS1 proteins (Figure 21). Sequence of the final candidate clone was analyzed (Table 5), which confirmed substitution of glycine to lysine. This new candidate clone was named after its mutation, 3B20-H1-13.

6. Specificity testing in the 2nd generation 3B20 scFv clone, 3B20-H1-13

To demonstrate the binding reactivity of 3B20-H1-13 scFv to ROS1, comparison experiments were performed with the 3B20 scFv in parallel. The 3B20-H1-13 scFv screened from site-directed mutagenesis NNK library showed improved specificity. Surprisingly, non-specific reactivity was no longer observed in the 3B20- H1-13 scFv (Figure 22A). Similar results were

obtained with immunoblots and pull-down assays (Figure 22B). Multiple bands resulting from non-specificity of the original scFv were removed when using the 3B20- H1-13 scFv. In addition, only single bands corresponding to the MW of the ROS1 protein was observed in pull-down assays, with the exception of the band corresponding to the 3B20-H1-13 scFv protein (approximately 55 kDa) bound to protein A agarose beads (Figure 22B).

7. Expression of the full-length wild type ROS1 protein in human lung cancer

To evaluate the applicability of the 3B20-H1-13 scFv in detection of the full-length wild type ROS1, immune-histochemistry (IHC) was performed in human lung adenocarcinoma and non-neoplastic tissue samples (N = 100). HEK 293T cells transfected with lentiviral vectors encoding the full-length 3B20-H1-13 scFv was used as positive controls; strong membranous and intracellular ROS1 expression was found (Figure 23A). Alveolar macrophages served as internal positive control; benign bronchial epithelia and alveolar pneumocytes were negative for ROS1 expression (Figure 23B).

Adenocarcinoma cells showed variable degrees of ROS1 expression, and strong positivity was found in approximately 10% of the cases. ROS1 was largely localized in intracellular membranes. However, intracellular ROS1 expression was also observed, especially in strong positive cases (Figure 23C–E). Some samples showed ROS1 expression in the membranes and intracellular with strong membranous accentuation (Figure 23F).

Table 1. Structure of ROS1 domains (Swiss-Prot Acc. P08922)

Amino acid residues No.	Domain
1 - 36	Signal peptide
101 - 196	Fibronectin Type-III 1
197 - 285	Fibronectin Type-III 2
291 - 513	6-bladed beta-propeller
557 - 671	Fibronectin Type-III 3
677 - 859	6-bladed beta-propeller
947 - 1042	Fibronectin Type-III 4
1043 - 1150	Fibronectin Type-III 5
1157 - 1416	6-bladed beta-propeller
1450 - 1556	Fibronectin Type-III 6
1557 - 1656	Fibronectin Type-III 7
1658 - 1751	Fibronectin Type-III 8
1752 - 1854	Fibronectin Type-III 9
1860 - 1882	Transmembrane

Table 2. Chicken immunization schedules

Antigen : ROS1 N-terminus (39~56) peptide conjugated with KLH					
	First injection	First boosting	Second boosting	Third boosting	Organ extraction
Ag amount	20 μg	20 μg	20 μg	20 μg	N/A
Day	First day	The 21st day	The 35th day	The 49th day	The 54st day
Products	Serum	Serum	Serum	Serum	Spleen Bursa of Fabricius Bone marrow Serum

Table 3. Primers for V_K and V_H of chicken scFv library with long linker

V_λ Primers		
CSCVK	(Sense)	CTG GCC CAG GCG GCC CTG ACT CAG CCG TCC TCG GTG TC
CKJo-B	(Reverse)	GGA AGA TCT AGA GGA CTG ACC TAG GAC GGT CAG G
V_H Primers		
CSCVHo-FL	(Sense)	GGT CAG TCC TCT AGA TCT TCC GGC GGT GGT GGC AGC TCC GGT GGT GGC GGT TCC GCC GTG ACG TT G GAC GAG
CSCG-B	(Reverse)	CTG GCC GGC CTG GCC ACT AGT GGA GGA GAC GAT GAC TTC GGT CC
Overlap Extension Primers		
CSC-F	(Sense)	GAG GAG GAG GAG GAG GAG GTG GCC CAG GCG GCC CTG ACT CAG
CSC-B	(Reverse)	GAG GAG GAG GAG GAG GAG GAG CTG GCC GGC CTG GCC ACT AGT GGA GG

Table 4. Results of bio-panning against the ROS1 peptides and recombinant ROS1 (37-290)-hFc fusion protein

	Chicken 1 (Library size : 8.7×10^9)		Chicken 2 (Library size : 5.9×10^9)		Chicken 3 (Library size : 7.2×10^9)			
	Input	**Output**	**Input**	**Output**	**Input**	**Output**	**Ag**	**Washing**
1st	7.0×10^{11}	6.4×10^6	3.0×10^{12}	1.5×10^7	3.0×10^{11}	1.1×10^7	N39-56-BSA	0.05% PBST x1
2nd	1.9×10^{12}	3.2×10^6	3.0×10^{11}	1.8×10^7	6.0×10^{11}	5.6×10^6	N39-56-OVA	0.05% PBST x3
3rd	1.9×10^{12}	6.4×10^6	1.0×10^{12}	1.4×10^8	7.0×10^{11}	9.0×10^7	N39-56-BSA	0.05% PBST x5
4th	1.0×10^{12}	6.6×10^7	8.9×10^{12}	8.6×10^7	6.0×10^{11}	1.5×10^8	N39-56-OVA	0.05% PBST x5
5th	1.0×10^{12}	2.2×10^7	9.0×10^{11}	8.6×10^7	1.2×10^{12}	1.4×10^8	ROS1(37-290)-hFc	0.05% PBST x5

Table 5. Lists of selected various anti-ROS1 scFv antibodies

R+H-*							
3B20	**G**	**G**	**G**	**G**	**N**	**I**	**D**	**A**
H1-30	**S**	G	G	G	N	I	D	A
H1-31	**N**	G	G	G	N	I	D	A
H1-13	**K**	G	G	G	N	I	D	A
H1-38	**N**	G	G	G	N	I	D	A
H1-42	**S**	G	G	G	N	I	D	A
H2-26	G	**N**	G	G	N	I	D	A
H2-36	G	**N**	G	G	N	I	D	A
H2-38	G	**S**	G	G	N	I	D	A
H3-28	G	G	**S**	G	N	I	D	A
H3-48	G	G	**S**	G	N	I	D	A
H3-19	G	G	**S**	G	N	I	D	A
H4-29	G	G	G	**A**	N	I	D	A
H4-44	G	G	G	**Y**	N	I	D	A
H4-03	G	G	G	**A**	N	I	D	A
H4-17	G	G	G	**S**	N	I	D	A
H5-45	G	G	G	G	**A**	I	D	A
H5-22	G	G	G	G	**G**	I	D	A
H5-02	G	G	G	G	**M**	I	D	A
H6-37	S	G	G	G	N	**L**	D	A
H6-29	G	G	G	G	N	**R**	D	A
H6-12	G	G	G	G	N	**G**	D	A
H6-25	G	G	G	G	N	**L**	D	A
H6-30	G	G	G	G	N	**R**	D	A

* R+H- clones binding to only ROS1

R+H+*							
3B20	**G**	**G**	**G**	**G**	**N**	**I**	**D**	**A**
H1-47	G	G	G	G	N	I	D	A
H1-48	G	G	G	G	N	I	D	A
H2-37	G	G	G	G	N	I	D	A
H2-21	G	G	G	G	N	I	D	A
H2-31	G	G	G	G	N	I	D	A
H3-45	G	G	G	G	N	I	D	A
H3-03	G	G	G	G	N	I	D	A
H3-44	G	G	G	G	N	I	D	A
H4-24	G	G	G	G	N	I	D	A
H4-05	G	G	G	G	N	I	D	A
H5-46	G	G	G	G	N	I	D	A
H5-44	G	G	G	G	N	I	D	A
H6-07	G	G	G	G	N	I	D	A
H6-28	G	G	G	G	N	I	D	A
H7-09	G	G	G	G	N	I	**S**	A
H8-18	G	G	G	G	N	I	D	A
H8-08	G	G	G	G	N	I	D	**K**

* R+H+ clones binding to both ROS1 and HSP

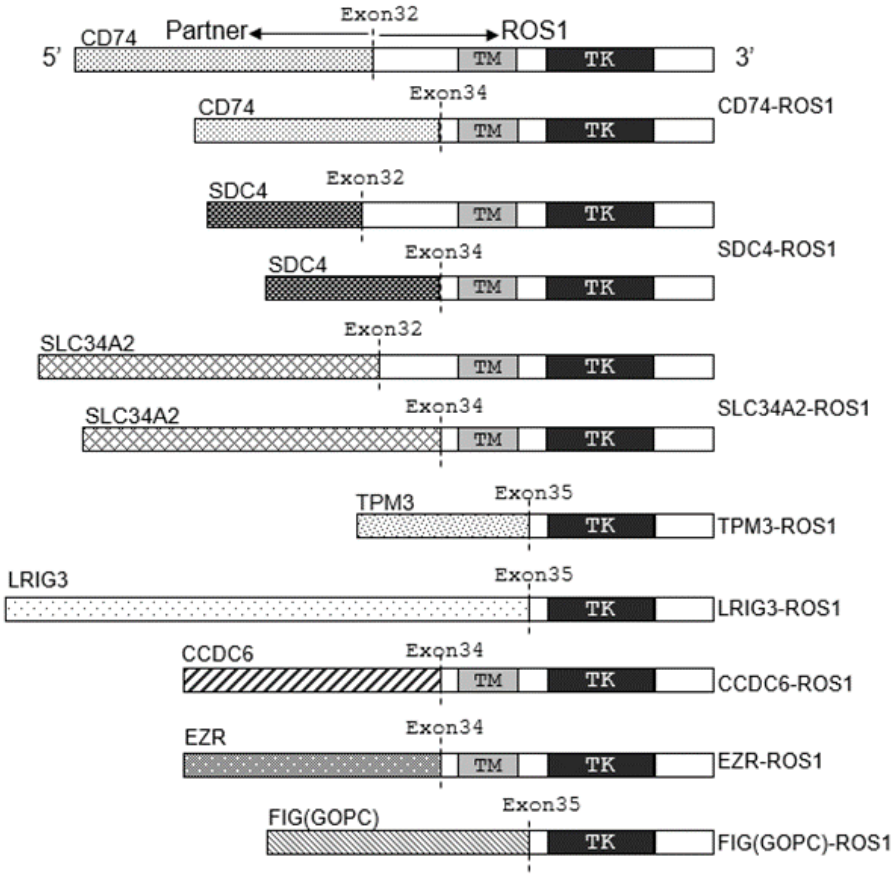

Figure 1. Various ROS1 rearrangements

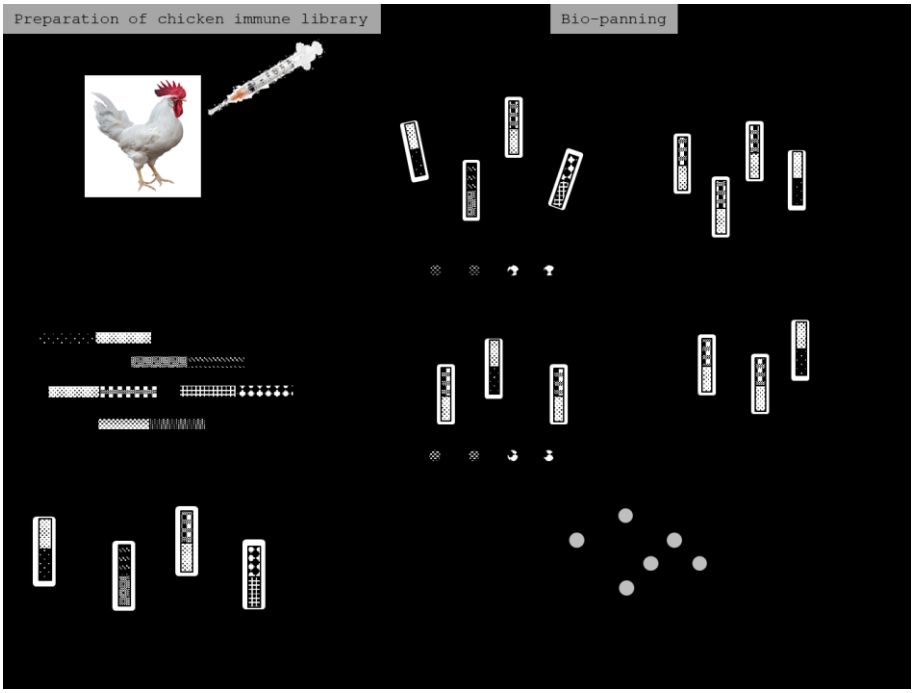

Figure 2. General schematic of bio-panning which is an affinity selection phage system

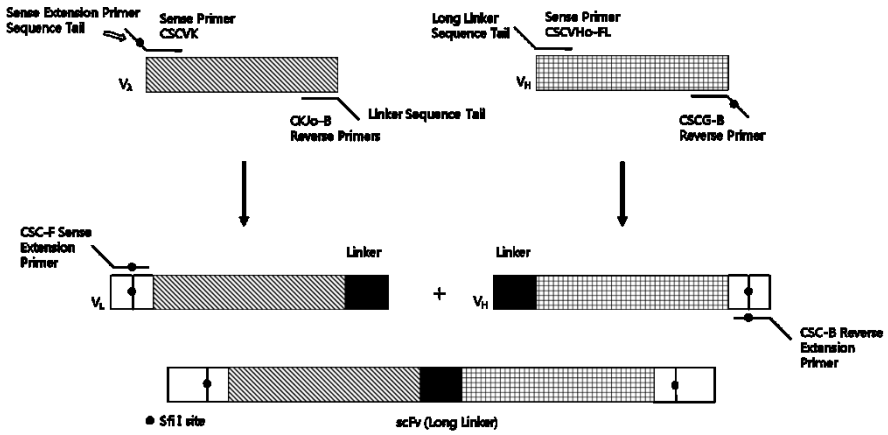

Figure 3. Construction of chicken scFv library

Chicken V_λ and V_H sequences were amplified for the construction of chicken scFv libraries. Each sense primer is combined with reverse primer to amplify gene segments from chicken cDNA. CSCVK and CSC-B have *Sfi* I restriction sites that are recognized by the extension primer in the overlap PCR. Primer CKJo-B and CSCVHo-FL have the sequence that corresponds to the long linker sequence that are used in the overlap extension PCR. The sense and reverse extension primers used in the second PCR recognize the sequence tails that were generated in the first round of PCR [21].

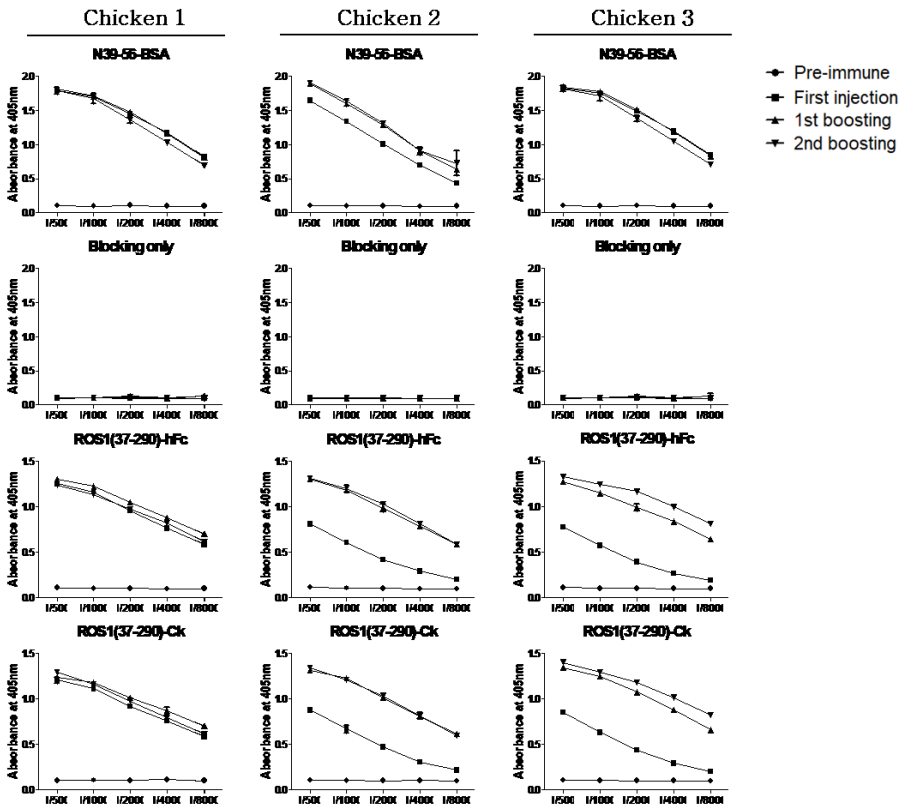

Figure 4. ELISA with ROS1 peptide immunized chicken serum

Three White Leghorn chickens were immunized with the ROS1 N-terminus (39~56) peptide conjugated with KLH. Serum was extracted from chicken blood and tested using ELISA for immunization titers.

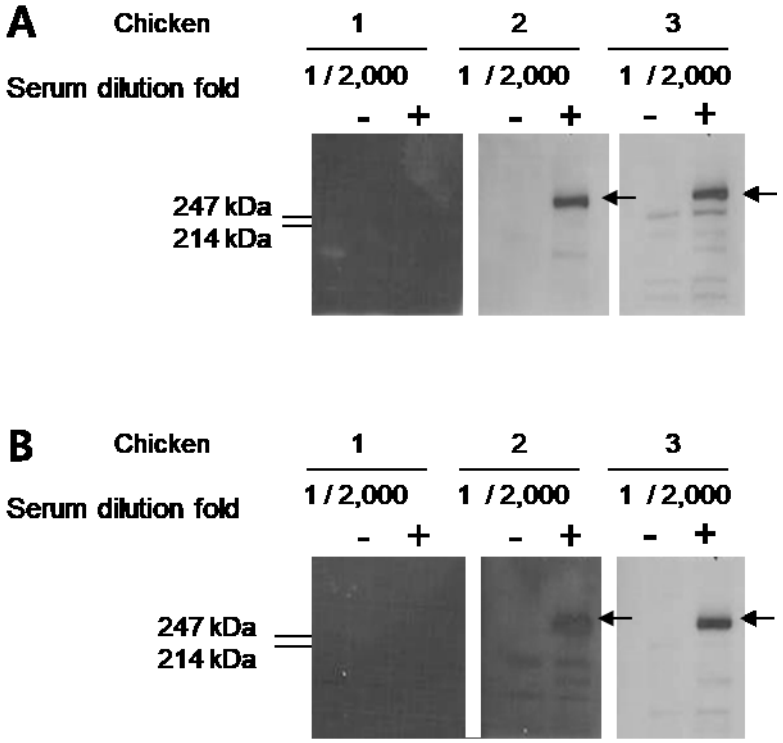

Figure 5. Immunoblots with ROS1 peptide immunized chicken serum

Immunoblots were performed to HEK 293T cells transfected with Lentiviral vector encoding human ROS1 cells using (A) 1st boosting serum and (B) 2nd boosting serum extracted from three immunized chicken's blood. Arrow indicates the 260 kDa molecular weight of full-length ROS1.

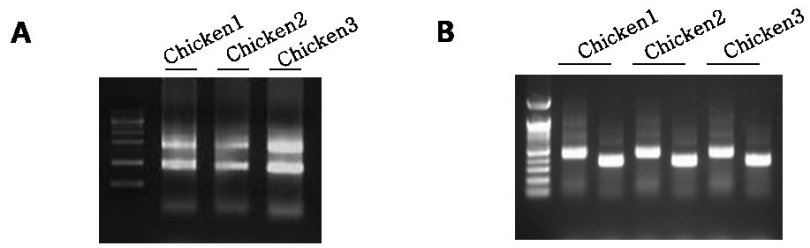

C

Test ligation results				
	Chicken 1	Chicken 2	Chicken 3	Strain
Library	3.4 x 10^8	1.6 x 10^8	1.7 x 10^8	
Stuffer		1.9 x 10^8		ER 2738
Self		1.2 x 10^6		

Figure 6. Construction of Chicken scFv libraries

(A) Total RNAs was extracted from immunized chicken's spleen, bursa of Fabricius and bone marrow. (B) First round of PCR was performed for V_H and V_λ amplifications. (C) The number of transformatants were calculated after test ligations.

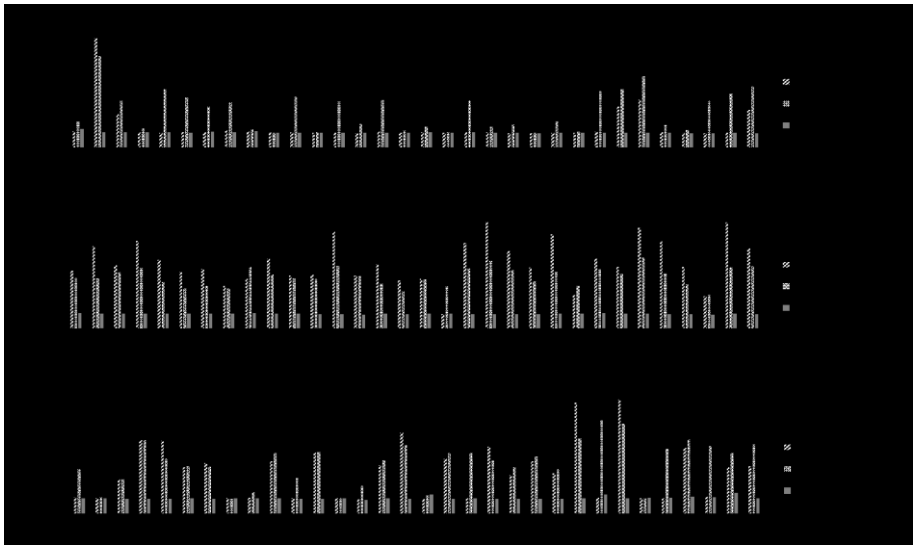

Figure 7. Phage ELISA results of 3rd bio-panning

A single colony from 3rd bio-panning out-put plates was cultured in SB media, and rescued phage was used for ROS1detection in an ELISA

Figure 8. Reactivity of the selected anti-ROS1 scFv antibody to ROS1

The binding affinity of the 3B20 scFv was measured by ELISA. The 3B20 scFv was prepared to (A) phage and (B) recombinant rFc fusion protein.

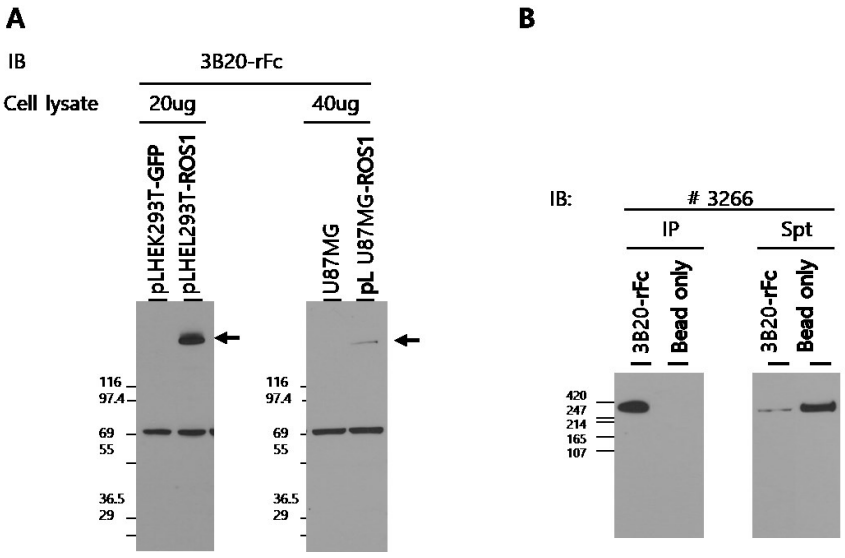

Figure 9. Reactivity of the selected anti-ROS1 scFv antibody to ROS1 in cell lysate

(A) Immunoblot analysis of the 3B20 scFv. Cell lysates of HEK 293T and U87MG cells transfected with lentiviral vector encoding ROS1, HEK 293T cells transfected GFP and wild type U87MG cells were subjected to SDS-PAGE. After transfer to nitrocellulose membranes and blocking, the membranes was probed with the 3B20 scFv-rFc fusion protein. (B) HEK 293T cells lentiviral transfected with ROS1 were lysed and incubated with the 3B20 scFv-rFc fusion protein and bound to protein A agarose beads. After washing steps, the protein bound to beads was eluted and subjected to SDS-PAGE and immunoblot assay

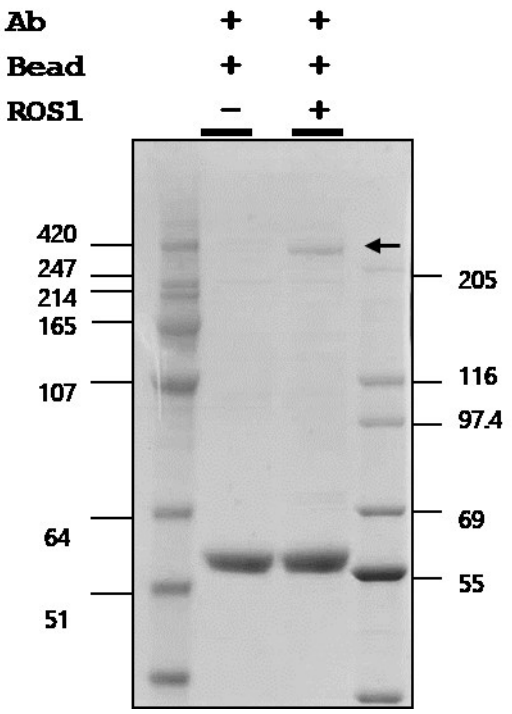

Figure 10. Pull-down assay of the 3B20 scFv

HEK 293T cells transfected with lentiviral vector encoding ROS1 were lysed and incubated with the 3B20 scFv-rFc fusion protein and bound to protein A agarose beads. After washing steps, the protein bound to beads was eluted and subjected to SDS-PAGE. Eluted proteins were stained with Coomassie Blue R250.

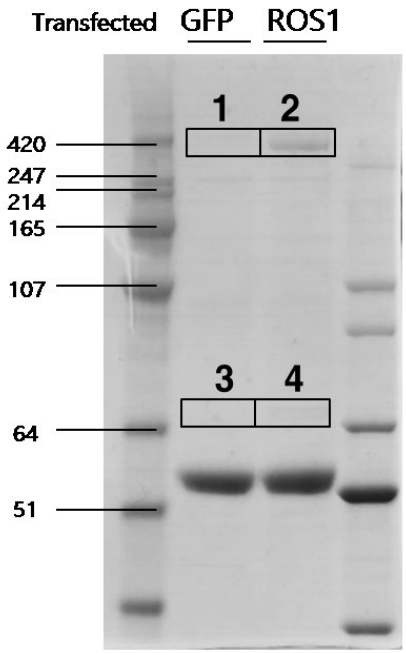

1

Identified Proteins	Transfected GFP
E3 ubiquitin-protein ligase UBR5	215
Isoform 2 of filamin-A	80
Isoform 1 of a-kinase anchor protein 13	34

2

Identified Proteins	Transfected ROS1
Proto-oncogene tyrosine-protein kinase ROS	390
E3 ubiquitin-protein ligase UBR5	216
Isoform 2 of filamin-A	97

3

Identified Proteins	Transfected GFP
Stress-70 protein, mitochondrial	134
Heat shock 70 kDa protein 1A/1B	102
Isoform 1 of heat shock cognate 71 kDa protein	83
78 kDa glucose-regulated protein	72
Isoform 1 of myotubularin-related prot ein 1	51

4

Identified Proteins	Transfected ROS1
78 kDa glucose-regulated protein	193
Stress-70 protein, mitochondrial	127
Heat shock 70 kDa protein 1A/1B	105
Isoform 1 of heat shock cognate 71 kDa protein	84
Isoform 1 of myotubularin-related prot ein 1	43

Figure 11. Lists of proteins identified by LC-MS/MS analysis

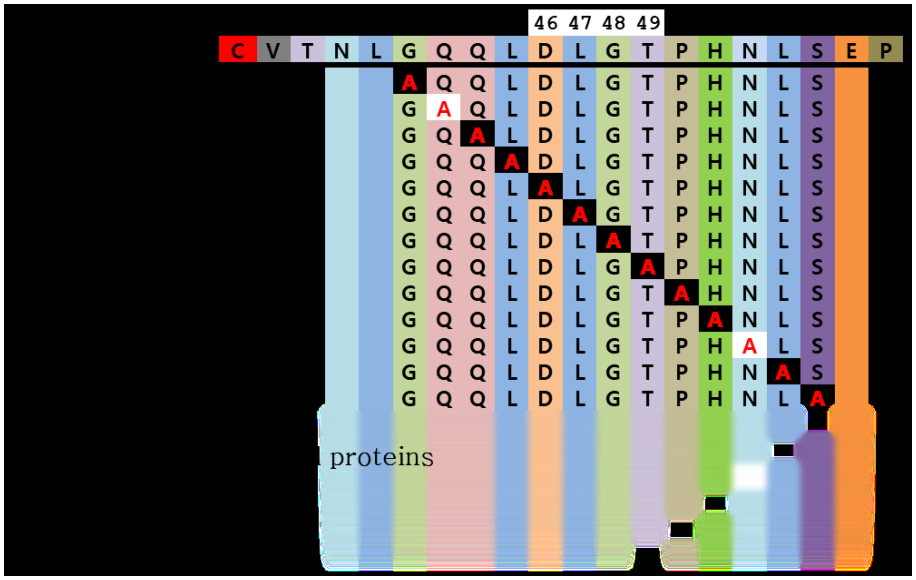

Figure 12. Schematic diagram of alanine scanning mutagenesis

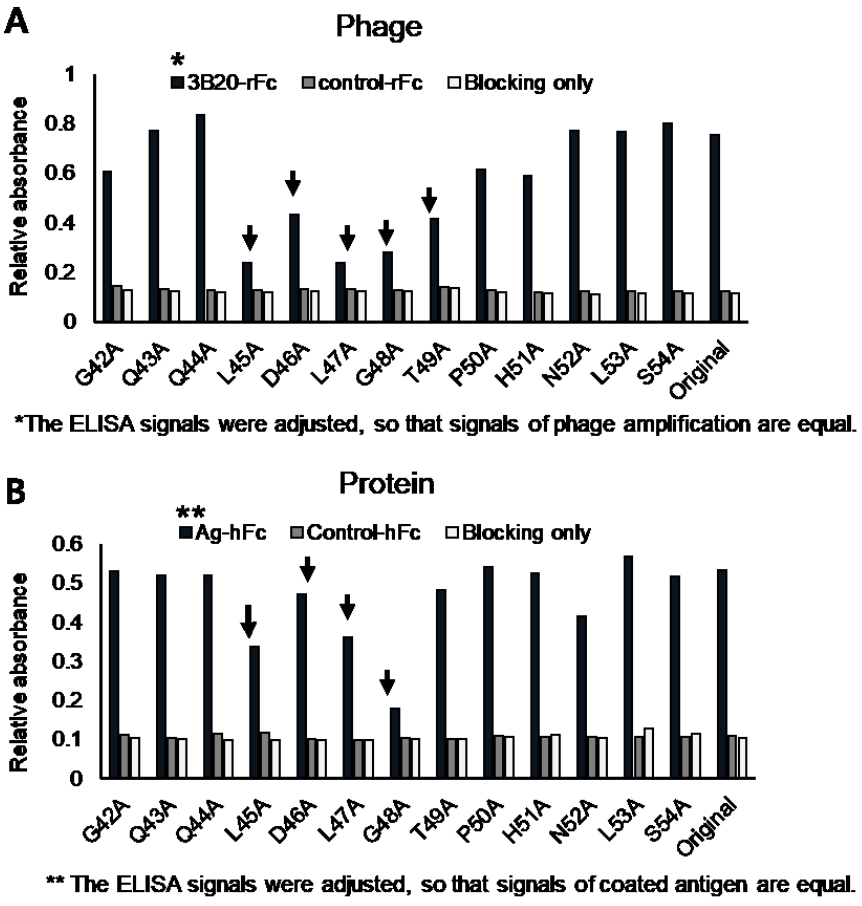

Figure 13. Reactivity of the alanine substituted recombinant ROS1 protein to the 3B20 scFv

(A) The 3B20 scFv-rFc fusion protein and the control-C_K protein were coated on 96 well microtiter plates. After blocking, ROS1 phages in which from 42 to 54 residue were replaced with alanine, respectively, were added. The amount of bound ROS1 phages were determined using HRP-conjugated anti-M13 antibody and ABTS solution. (B) Recombinant ROS1-hFc fusion

protein which is substituted alanine were coated on 96 well microtiter plates. After blocking, the 3B20 scFv-C_K fusion protein was added, respectively. The amount of bound the anti-ROS1 scFv antibody was determined using HRP-conjugated anti-C_K antibody and ABTS solution.

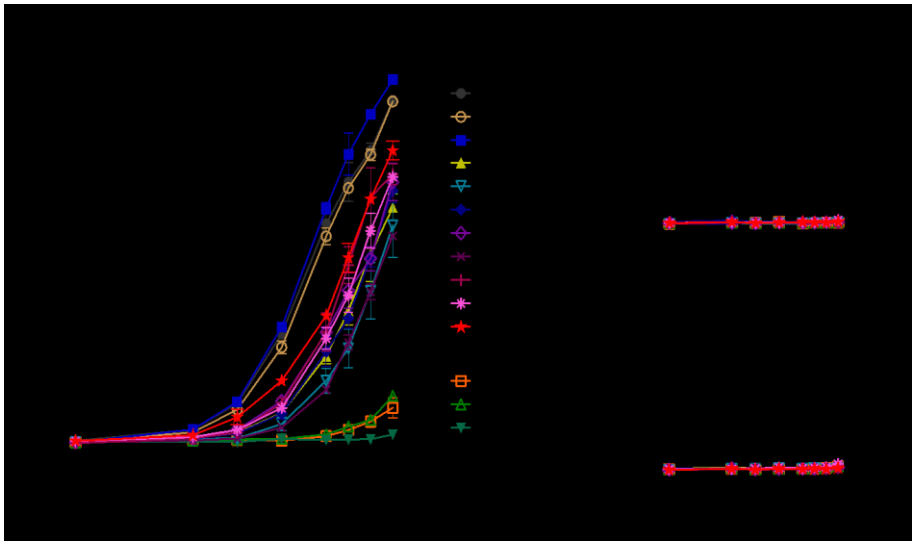

Figure 14. Identification of the 3B20 scFv epitope by alanine scanning mutagenesis

The wells of microtiter plates were coated with the 3B20 scFv-C_K fusion protein (A), BSA (B), or an irrelevant scFv-C_K fusion protein (C). The plates were incubated with alanine substituted ROS1-hFc fusion proteins or wild type ROS1-hFc fusion protein in a dose dependent manner. The amounts of bound ROS1-hFc fusion proteins were determined using an HRP-conjugated anti-hFc antibody and ATBS solution.

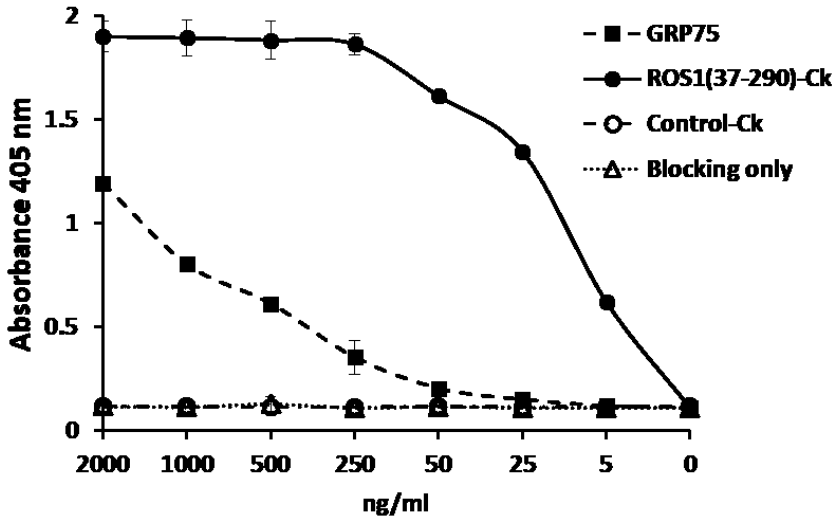

Figure 15. Reactivity of the 3B20 scFv to ROS1 and Hsp70 (GRP75)

Recombinant ROS1 (amino acids 37-290)-C_K fusion protein, GRP75 and control-C_K protein were coated on 96 well microtiter plates. After blocking, the 3B20 scFv-rFc fusion protein was added. The amount of bound antibody was determined using HRP-conjugated anti-rabbit IgG antibody and ABTS solution.

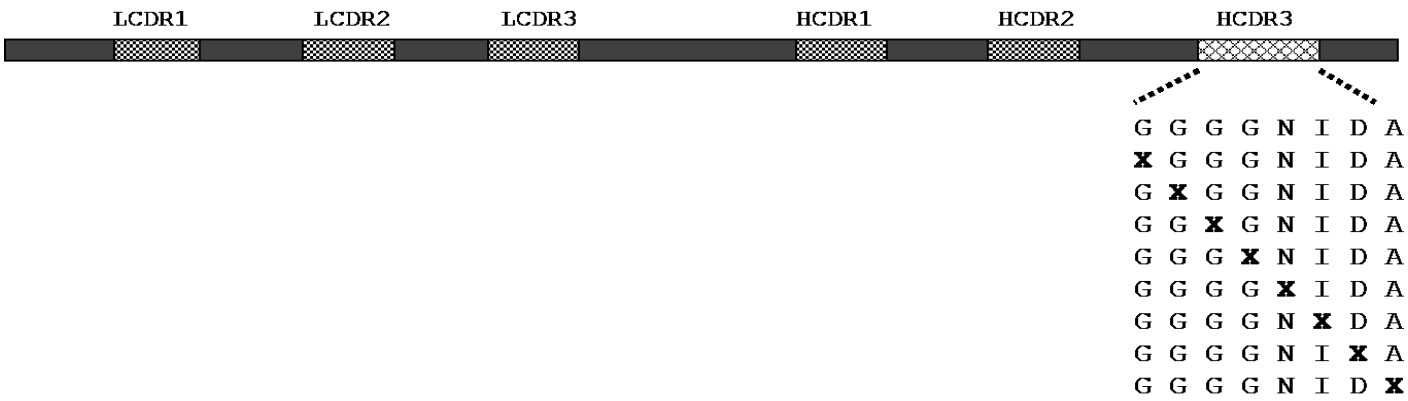

Figure 16. Schematic of HCDR3 site-directed mutagenesis libraries in the 3B20 scFv

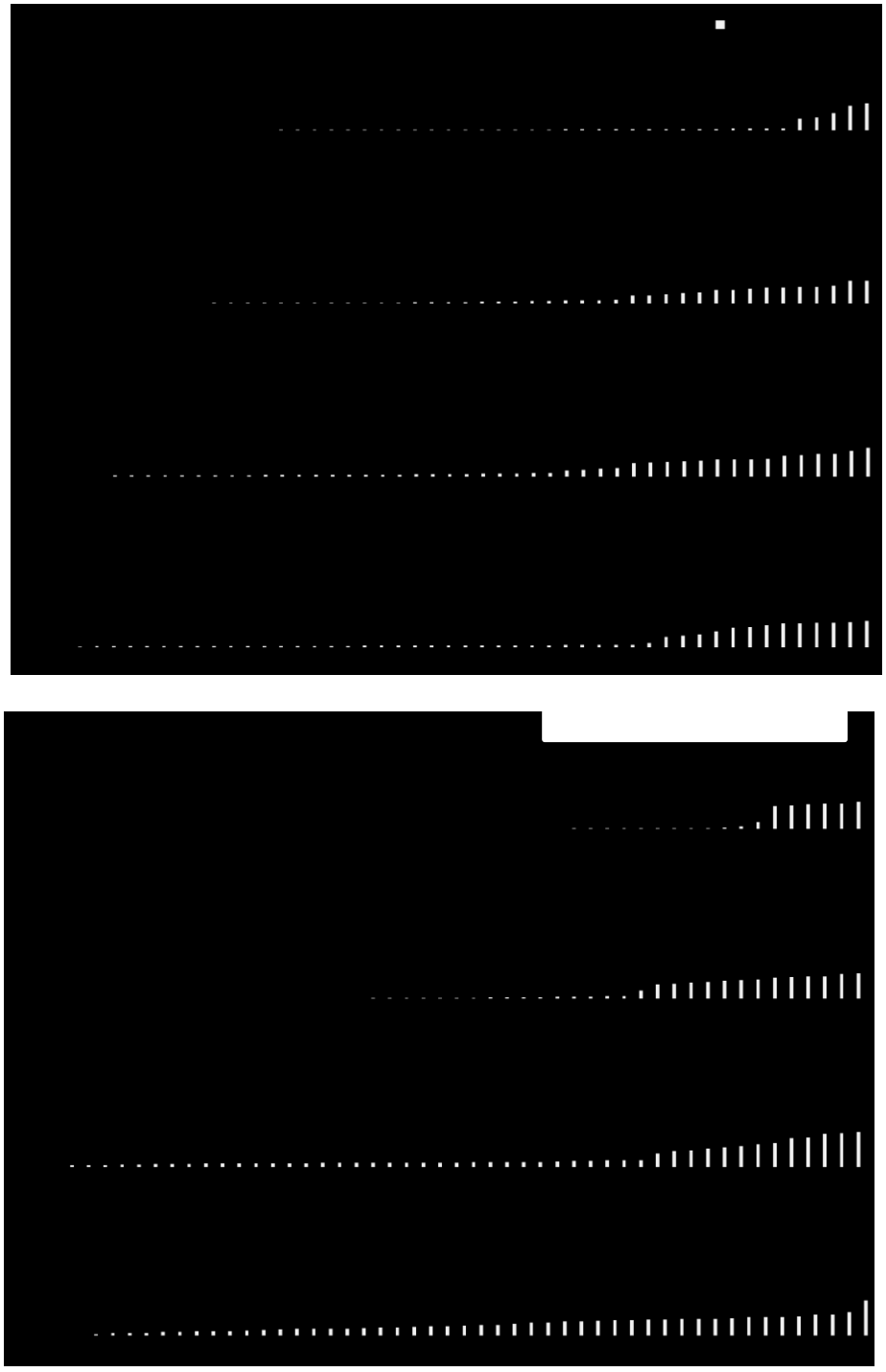

Figure 17. Reactivity of site-directed HCDR3 libraries of the 3B20 scFv to ROS1 and GRP75

Recombinant ROS1 (amino acids 37-290)-hFc fusion protein, GRP75 were coated on 96 well microtiter plates. After blocking, the 3B20 scFv-C_K fusion protein was added, respectively. The amount of bound phage was determined using HRP-conjugated anti-M13 antibody and ABTS solution. Blank results were subtracted from the reading for all other wells, then ELISA graphs were described in ascending order based on the GRP75 signals. The original clones were marked by a square box.

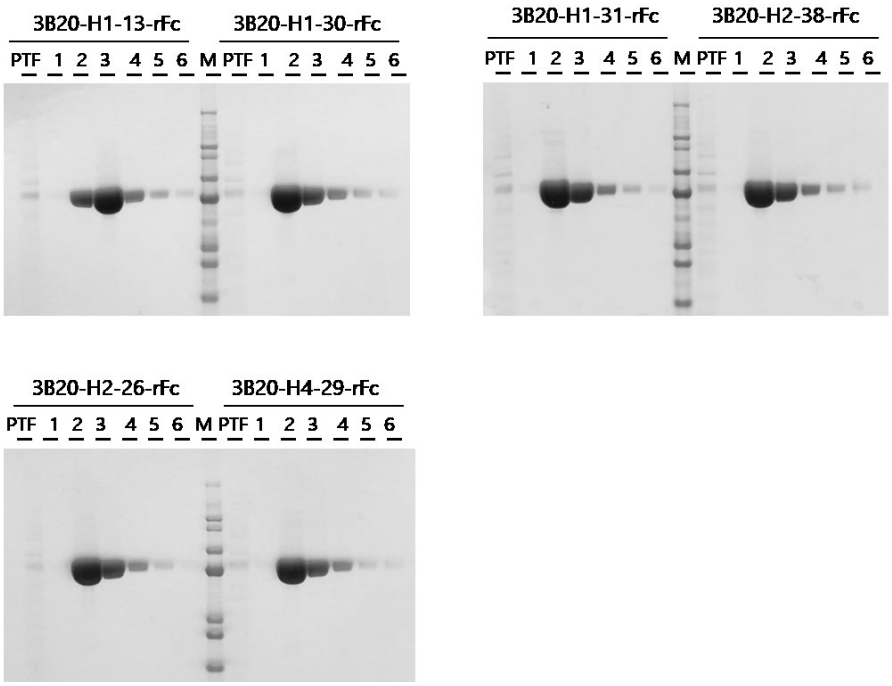

Figure 18. Overexpression and purification of anti-ROS1 scFv antibodies

HEK 293F cells were transfected with selected anti-ROS1 scFv clones from site-directed HCDR3 libraries of the 3B20 scFv. After purification using protein A agarose beads, and purified proteins were confirmed by SDS-PAGE and Coomassie Blue R250 staining.

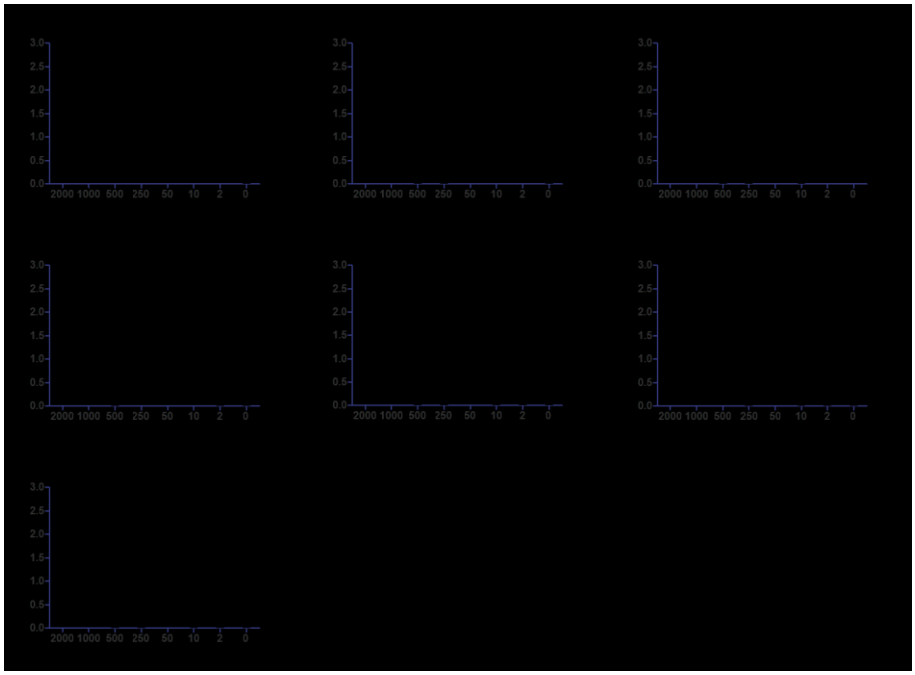

Figure 19. Reactivity of selected anti-ROS1 scFv antibodies from site-directed HCDR3 libraries of the 3B20 scFv to ROS1 and GRP75

Recombinant ROS1 (amino acids 37-290)-C_K fusion protein, GRP75 and Control- C_K fusion protein were coated on 96 well microtiter plates. After blocking, the 3B20 scFv-rFc fusion protein was added. The amount of bound antibody was determined using HRP-conjugated anti-rFc antibody and ABTS solution.

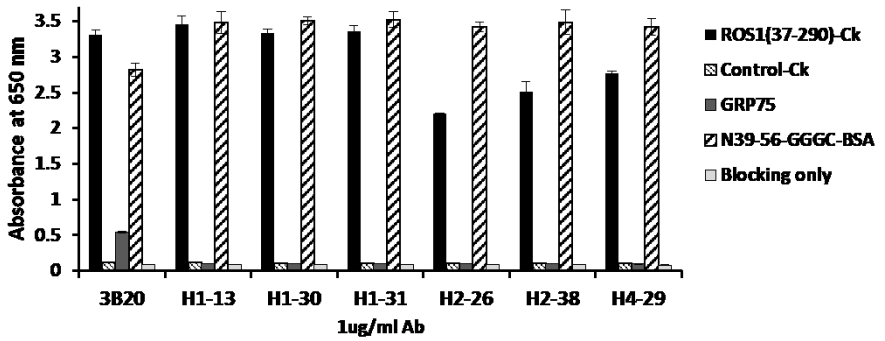

Figure 20. Reactivity of selected anti-ROS1 scFv antibodies from site-directed HCDR3 libraries of the 3B20 scFv to ROS1 peptide

Recombinant ROS1 (amino acids 37-290)-C_K fusion protein, GRP75, Control- C_K fusion protein and ROS1 N-terminus (39~56) peptide conjugated with BSA were coated on 96 well microtiter plates. After blocking, the 3B20 scFv-rFc fusion protein was added. The amount of bound antibody was determined using HRP-conjugated anti-rFc antibody and TMB solution.

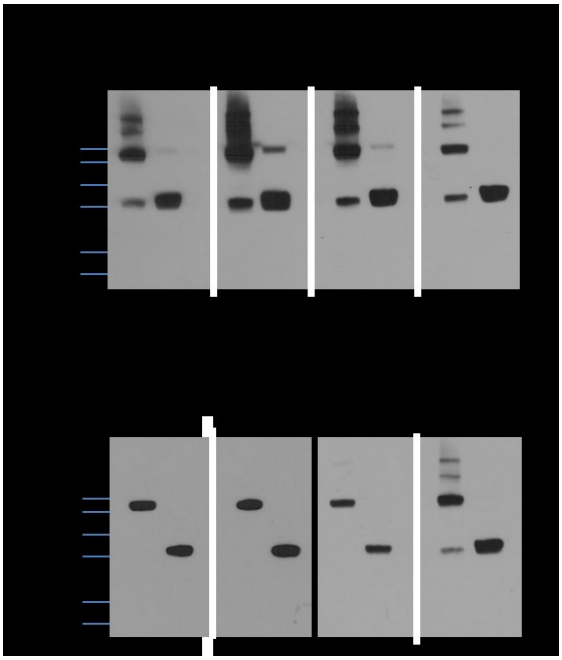

Figure 21. Immunoblot analysis of selected anti-ROS1 scFv antibodies from site-directed HCDR3 libraries of the 3B20 scFv

Recombinant ROS1 (37-290)-C_K fusion protein was loaded in non-reduced condition (NP) and reduced condition (R) in SDS-PAGE and transferred onto nitrocellulose membranes. After blocking, the 3B20 scFv-rFc fusion protein and clones derived 3B20 scFv were incubated with membranes. HRP-conjugated anti-rFc antibody and chemiluminescent substrate were used for visualization of the bands. The ab5512 was used by positive control antibody for detection of ROS1.

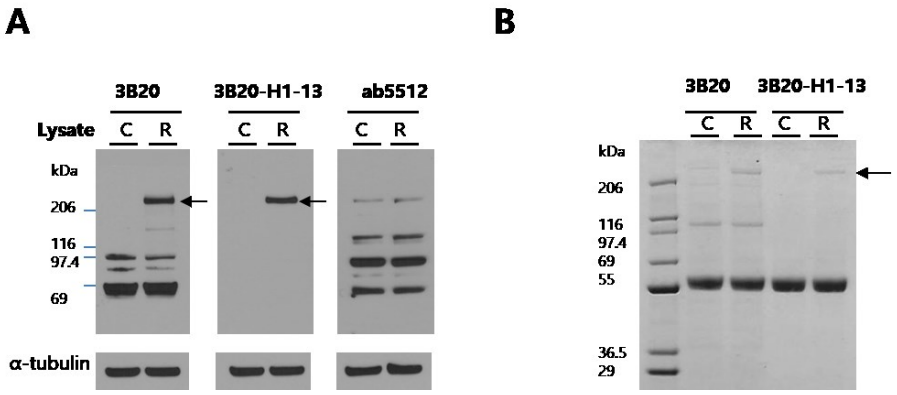

Figure 22. Specificity of 3B20 scFv and 3B20-H1-13 scFv

(A) Cell lysates of HEK 293T cells transfected with lentiviral vector encoding ROS1 (lane R) or a control vector (lane C) were subjected to SDS-PAGE. After transfer to nitrocellulose membranes and blocking, the membraned were probed with antibodies, 3B20 scFv, 3B20-H1-13 scFv, or ROS1 (ab5515). Full-length ROS1 (arrow) was detected in lysates from cells transfected with ROS1. (B) HEK 293T cells transfected with GFP or ROS1 were lysed and incubated with 3B20 scFv and 3B20-H1-13 scFv fused to rFc and bound to protein A agarose beads. After washing, the protein bound to beads was eluted and subjected to SDS-PAGE. The protein bands were visualized using Coomassie Blue R250.

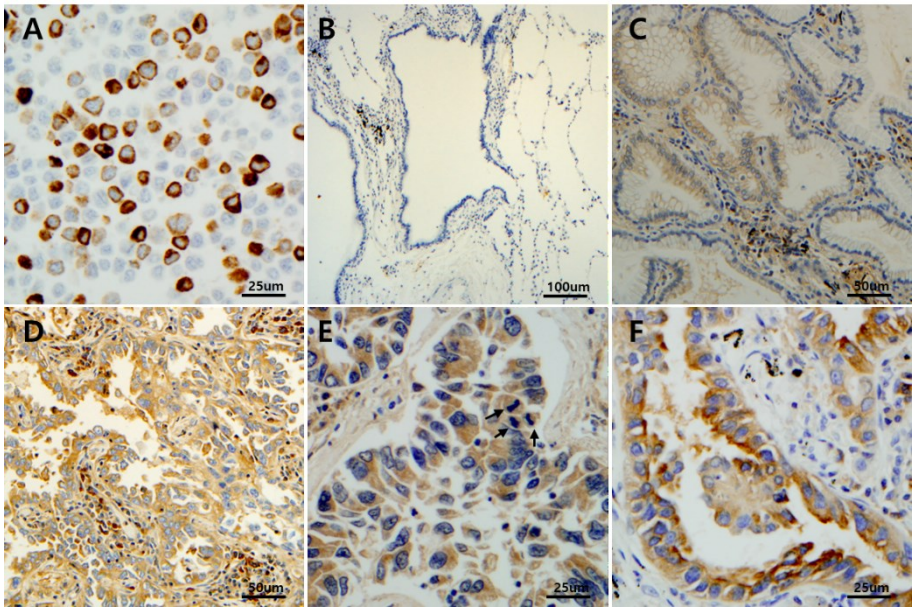

Figure 23. Results of immunohistochemistry with 3B20-H1-13 scFv

(A) HEK 293T cells transfected with lentiviral vector encoding human ROS1 (full-length) showed strong expression of ROS1 in the intracellular membrane and also in the cytoplasm (x400). (B) Non-neoplastic lung tissue was negative for ROS1 (x100). (C-E) Expression of ROS1 was found in adenocarcinoma of the lung, in low levels (C x200), intermediate to high levels (D x200), and high levels (E x400; arrows show mitotic figures). (F) ROS1-positive IHC was found in the intracellular membranes and cytoplasm of the tumor cells, with accentuation of membranous expression (x400).

DISCUSSION

The proto-oncogene tyrosine kinase ROS1 has been considered to be a cancer-specific target molecule in both clinical and academic fields. So far, researchers have mainly focused on studying ROS1 rearrangements, ROS1 fusion proteins, and ROS1 inhibitors. For example, the small molecule crizotinib (trade name Xalkori, Pfizer) is a representative ROS1 inhibitor that targets the C-terminus of the ROS1 fusion protein. However, studies on the full-length wild type ROS1 have not yet been fully established. Commercial anti-ROS1 antibodies have been developed. However, these antibodies mainly target the C-terminal epitope of the ROS1 protein. ROS1 fusion proteins possess a 3′ region of ROS1 and a 5′ region from another partner. Hence, most commercially available antibodies target the C-terminus of ROS1. These antibodies cannot identify, or be used for full-length ROS1 investigation. For example, the recently developed D4D6 is a good quality anti-ROS1 rabbit mAb that binds to the C-terminal epitope of ROS1. In addition, commercially available anti-ROS1 antibodies with N-terminal recognition site are very expensive and rare. Again, my preliminary test results demonstrated poor affinity and

specificity of these commercial antibodies as N-terminal ROS1 target antibodies. Therefore, modified anti-ROS1 mAbs that exhibit enhanced specificity to the N-terminus of ROS1 have developed.

The majority of ROS1-expressing cells have been reported to possess ROS1 fusion proteins, whereas cell expressing the full-length ROS1 has not been found. Rimkunas et al. have previously reported that they were unable to identify cells expressing the full-length ROS1. My study has also attempted to isolate the full-length ROS1 in various cell lines. However, despite my many attempts, the full-length wild type ROS1 was not observed in any cell lines, except in lentivirus- infected cells. Recent studies suggested that ROS1 expression is higher in recurring tumors as compared with that in primary tumors. In addition, it has been reported that methylation inhibitors reduce ROS1 promoter methylation, which leads to increased ROS1 expression. It was hypothesized that ROS1 expression is blocked under normal conditions, and that its expression is under epigenetic regulation.

Based on my knowledge, this is the first study that showcases successful generation of the full-length ROS1 protein; the full-length ROS1 protein was produced with developed expression system using the lentiviral vector. My study then developed the anti-ROS1 scFv antibody and 3B20, which demonstrated high reactivity and specificity for the target molecule as compared with commercial antibodies. Furthermore, my study was delineated epitope amino acid residues within the ROS1 proteins that play a critical role in the recognition of the 3B20 scFv. However, non-specific reactivity of the 3B20 scFv was detected in mass spectroscopy, immunoblots, and pull-down assays. The 3B20 scFv binds to ROS1 with higher affinity as compared with that of commercial anti-ROS1 antibodies (ab5512). However, when using the 3B20 scFv, multiple specific bands were detected in immunoblot and pull-down assays. These multiple specific bands appeared at 70 kDa, which mass spectrometry revealed to be Hsp70s. Protein homology analysis indicated that the Hsp70s family shares the same binding sequence as ROS1. Hence, in this study was further investigated and verified that a member of the Hsp70s family, GRP75, can also bind to 3B20 scFv. GRP75 was commercially purchased, and binding reactivity of GRP75 was

measured using ELISA. As expected, GRP75 was able to bind to the 3B20 scFv. Therefore, elimination of non-specific binding is necessary to obtain high quality 3B20 scFv.

Subsequently, my study tried to improve specificity of the 3B20 scFv without losing its affinity for ROS1. The heavy chain complementarity-determining region 3 (HCDR3) is known to be the most important region for antibody-antigen interactions, and is associated with poly-reactivity. Thus, substitution within the HCDR3 region was carried out to alter its specificity. It is possible that substituted amino acids may not affect antibody-antigen interactions. Indeed, studying individual HCDR3 site-directed mutagenesis libraries will help us understand what residues are responsible for antibody-antigen interactions. This will be valuable for determining which residue is the best option for substitution, or which amino acid in HCDR3 is critical for antigen-antibody interactions.

In summary, an anti-ROS1 N-terminal binding scFv antibody was successfully developed, and an individual NNK library of each amino acid position in the HCDR3 region have constructed to improve specificity of the clone. Although, a cell line that

expressed the full-length wild type ROS1 was not found, cells that expressed the full-length ROS1 protein using lentiviral vectors were generated. In this study, single amino acid changes in HCDR3 induced antibody binding specificity were demonstrated. Finally, an anti-ROS1 scFv antibody was developed and modified to show its potential for investigating the full-length ROS1. My opinion is that further studies on ROS1 using this clone would reveal uncovered biological functions of the full-length ROS1.

REFERENCES

[1] M.D. Abeloff, Abeloff's clinical oncology, 4th ed., Churchill Livingstone/Elsevier, Philadelphia, 2008.

[2] S. Novello, F. Barlesi, R. Califano, T. Cufer, S. Ekman, M.G. Levra, K. Kerr, S. Popat, M. Reck, S. Senan, G.V. Simo, J. Vansteenkiste, S. Peters, E.G. Committee, Metastatic non-small-cell lung cancer: ESMO Clinical Practice Guidelines for diagnosis, treatment and follow-up, Ann Oncol, 27 (2016) v1-v27.

[3] P.C. Ma, R. Jagadeeswaran, S. Jagadeesh, M.S. Tretiakova, V. Nallasura, E.A. Fox, M. Hansen, E. Schaefer, K. Naoki, A. Lader, W. Richards, D. Sugarbaker, A.N. Husain, J.G. Christensen, R. Salgia, Functional expression and mutations of c-Met and its therapeutic inhibition with SU11274 and small interfering RNA in non-small cell lung cancer, Cancer Res, 65 (2005) 1479-1488.

[4] J.J. Lin, A.T. Shaw, Resisting Resistance: Targeted Therapies in Lung Cancer, Trends Cancer, 2 (2016) 350-364.

[5] J. Soh, S. Toyooka, K. Matsuo, H. Yamamoto, Wistuba, II, S. Lam, K.M. Fong, A.F. Gazdar, S. Miyoshi, Ethnicity affects EGFR and KRAS gene alterations of lung adenocarcinoma, Oncol Lett, 10 (2015) 1775-1782.

[6] M. Maemondo, A. Inoue, K. Kobayashi, S. Sugawara, S. Oizumi, H. Isobe, A. Gemma, M. Harada, H. Yoshizawa, I. Kinoshita, Y. Fujita, S. Okinaga, H. Hirano, K. Yoshimori, T. Harada, T. Ogura, M. Ando, H. Miyazawa, T. Tanaka, Y. Saijo, K. Hagiwara, S. Morita, T. Nukiwa, G. North-East Japan Study, Gefitinib or chemotherapy for non-small-cell lung cancer with mutated EGFR, N Engl J Med, 362 (2010) 2380-2388.

[7] H. Matsushime, L.H. Wang, M. Shibuya, Human c-ros-1 gene homologous to the v-ros sequence of UR2 sarcoma virus encodes for a transmembrane receptorlike molecule, Mol Cell Biol, 6 (1986) 3000-3004.

[8] M. Rabin, D. Birnbaum, D. Young, C. Birchmeier, M. Wigler, F.H. Ruddle, Human ros1 and mas1 oncogenes located in regions of chromosome 6 associated with tumor-

specific rearrangements, Oncogene Res, 1 (1987) 169-178.

[9] C. Birchmeier, S. Sharma, M. Wigler, Expression and rearrangement of the ROS1 gene in human glioblastoma cells, Proc Natl Acad Sci U S A, 84 (1987) 9270-9274.

[10] S.M. Jong, L.H. Wang, Two point mutations in the transmembrane domain of P68gag-ros inactive its transforming activity and cause a delay in membrane association, J Virol, 65 (1991) 180-189.

[11] H. Verbeek, G. Meyer, D. Challis, A. Zabalegui, M.E. Soto, K. Saks, H. Leino-Kilpi, S. Karlsson, J.P. Hamers, C. RightTimePlaceCare, Inter-country exploration of factors associated with admission to long-term institutional dementia care: evidence from the RightTimePlaceCare study, J Adv Nurs, 71 (2015) 1338-1350.

[12] K. Bergethon, A.T. Shaw, S.H. Ou, R. Katayama, C.M. Lovly, N.T. McDonald, P.P. Massion, C. Siwak-Tapp, A. Gonzalez, R. Fang, E.J. Mark, J.M. Batten, H. Chen, K.D. Wilner, E.L. Kwak, J.W. Clark, D.P. Carbone, H. Ji, J.A.

Engelman, M. Mino-Kenudson, W. Pao, A.J. Iafrate, ROS1 rearrangements define a unique molecular class of lung cancers, J Clin Oncol, 30 (2012) 863-870.

[13] K. Rikova, A. Guo, Q. Zeng, A. Possemato, J. Yu, H. Haack, J. Nardone, K. Lee, C. Reeves, Y. Li, Y. Hu, Z. Tan, M. Stokes, L. Sullivan, J. Mitchell, R. Wetzel, J. Macneill, J.M. Ren, J. Yuan, C.E. Bakalarski, J. Villen, J.M. Kornhauser, B. Smith, D. Li, X. Zhou, S.P. Gygi, T.L. Gu, R.D. Polakiewicz, J. Rush, M.J. Comb, Global survey of phosphotyrosine signaling identifies oncogenic kinases in lung cancer, Cell, 131 (2007) 1190-1203.

[14] K. Takeuchi, M. Soda, Y. Togashi, R. Suzuki, S. Sakata, S. Hatano, R. Asaka, W. Hamanaka, H. Ninomiya, H. Uehara, Y. Lim Choi, Y. Satoh, S. Okumura, K. Nakagawa, H. Mano, Y. Ishikawa, RET, ROS1 and ALK fusions in lung cancer, Nat Med, 18 (2012) 378-381.

[15] K.D. Davies, A.T. Le, M.F. Theodoro, M.C. Skokan, D.L. Aisner, E.M. Berge, L.M. Terracciano, F. Cappuzzo, M. Incarbone, M. Roncalli, M. Alloisio, A. Santoro, D.R.

Camidge, M. Varella-Garcia, R.C. Doebele, Identifying and targeting ROS1 gene fusions in non-small cell lung cancer, Clin Cancer Res, 18 (2012) 4570-4579.

[16] V.M. Rimkunas, K.E. Crosby, D. Li, Y. Hu, M.E. Kelly, T.L. Gu, J.S. Mack, M.R. Silver, X. Zhou, H. Haack, Analysis of receptor tyrosine kinase ROS1-positive tumors in non-small cell lung cancer: identification of a FIG-ROS1 fusion, Clin Cancer Res, 18 (2012) 4449-4457.

[17] T.L. Gu, X. Deng, F. Huang, M. Tucker, K. Crosby, V. Rimkunas, Y. Wang, G. Deng, L. Zhu, Z. Tan, Y. Hu, C. Wu, J. Nardone, J. MacNeill, J. Ren, C. Reeves, G. Innocenti, B. Norris, J. Yuan, J. Yu, H. Haack, B. Shen, C. Peng, H. Li, X. Zhou, X. Liu, J. Rush, M.J. Comb, Survey of tyrosine kinase signaling reveals ROS kinase fusions in human cholangiocarcinoma, PLoS One, 6 (2011) e15640.

[18] Y. Jin, P.L. Sun, H. Kim, E. Park, H.S. Shim, S. Jheon, K. Kim, C.T. Lee, J.H. Chung, ROS1 gene rearrangement and copy number gain in non-small cell lung cancer, Virchows Arch, 466 (2015) 45-52.

[19] J. Acquaviva, R. Wong, A. Charest, The multifaceted roles of the receptor tyrosine kinase ROS in development and cancer, Biochim Biophys Acta, 1795 (2009) 37-52.

[20] G.P. Smith, Filamentous fusion phage: novel expression vectors that display cloned antigens on the virion surface, Science, 228 (1985) 1315-1317.

[21] C.F. Barbas, Phage display : a laboratory manual, Cold Spring Harbor Laboratory Press, Cold Spring Harbor, NY, 2001.

[22] W.A. Clark, W. Horneland, A.G. Klein, Attempts to freeze some bacteriophages to ultralow temperatures, Appl Microbiol, 10 (1962) 463-465.

[23] E. Jonczyk, M. Klak, R. Miedzybrodzki, A. Gorski, The influence of external factors on bacteriophages--review, Folia Microbiol (Praha), 56 (2011) 191-200.

[24] S.D. Branston, E.C. Stanley, J.M. Ward, E. Keshavarz-Moore, Determination of the survival of bacteriophage M13 from chemical and physical challenges to assist in its sustainable bioprocessing, Biotechnol Bioproc E, 18 (2013)

560-566.

[25] G. Walter, Z. Konthur, H. Lehrach, High-throughput screening of surface displayed gene products, Comb Chem High Throughput Screen, 4 (2001) 193-205.

[26] H. Hawlisch, M. Muller, R. Frank, W. Bautsch, A. Klos, J. Kohl, Site-specific anti-C3a receptor single-chain antibodies selected by differential panning on cellulose sheets, Anal Biochem, 293 (2001) 142-145.

[27] W. Noppe, F. Plieva, I.Y. Galaev, H. Pottel, H. Deckmyn, B. Mattiasson, Chromato-panning: an efficient new mode of identifying suitable ligands from phage display libraries, BMC Biotechnol, 9 (2009) 21.

[28] M. Hust, E. Maiss, H.J. Jacobsen, T. Reinard, The production of a genus-specific recombinant antibody (scFv) using a recombinant potyvirus protease, J Virol Methods, 106 (2002) 225-233.

[29] B. Krebs, R. Rauchenberger, S. Reiffert, C. Rothe, M. Tesar, E. Thomassen, M. Cao, T. Dreier, D. Fischer, A. Hoss, L. Inge, A. Knappik, M. Marget, P. Pack, X.Q. Meng,

R. Schier, P. Sohlemann, J. Winter, J. Wolle, T. Kretzschmar, High-throughput generation and engineering of recombinant human antibodies, J Immunol Methods, 254 (2001) 67-84.

[30] C. Lombard-Banek, E.P. Portero, R.M. Onjiko, P. Nemes, New-generation mass spectrometry expands the toolbox of cell and developmental biology, Genesis, 55 (2017).

[31] L. Huang, J. Lu, V.J. Wroblewski, J.M. Beals, R.M. Riggin, In vivo deamidation characterization of monoclonal antibody by LC/MS/MS, Anal Chem, 77 (2005) 1432-1439.

[32] Z. Zhang, H. Pan, X. Chen, Mass spectrometry for structural characterization of therapeutic antibodies, Mass Spectrom Rev, 28 (2009) 147-176.

[33] D. Nebija, H. Kopelent-Frank, E. Urban, C.R. Noe, B. Lachmann, Comparison of two-dimensional gel electrophoresis patterns and MALDI-TOF MS analysis of therapeutic recombinant monoclonal antibodies trastuzumab and rituximab, J Pharm Biomed Anal, 56 (2011)

684-691.

[34] S. Kamoda, R. Ishikawa, K. Kakehi, Capillary electrophoresis with laser-induced fluorescence detection for detailed studies on N-linked oligosaccharide profile of therapeutic recombinant monoclonal antibodies, J Chromatogr A, 1133 (2006) 332-339.

[35] G. Maccarrone, J.J. Bonfiglio, S. Silberstein, C.W. Turck, D. Martins-de-Souza, Characterization of a Protein Interactome by Co-Immunoprecipitation and Shotgun Mass Spectrometry, Methods Mol Biol, 1546 (2017) 223-234.

[36] G.C. Hadlock, C.C. Nelson, A.J. Baucum, 2nd, G.R. Hanson, A.E. Fleckenstein, Ex vivo identification of protein-protein interactions involving the dopamine transporter, J Neurosci Methods, 196 (2011) 303-307.

[37] T.I. Milac, T.W. Randolph, P. Wang, Analyzing LC-MS/MS data by spectral count and ion abundance: two case studies, Stat Interface, 5 (2012) 75-87.

[38] K.A. Neilson, N.A. Ali, S. Muralidharan, M. Mirzaei, M. Mariani, G. Assadourian, A. Lee, S.C. van Sluyter, P.A.

Haynes, Less label, more free: approaches in label-free quantitative mass spectrometry, Proteomics, 11 (2011) 535-553.

[39] M. Baker, Reproducibility crisis: Blame it on the antibodies, Nature, 521 (2015) 274-276.

[40] L. Berglund, E. Bjorling, P. Oksvold, L. Fagerberg, A. Asplund, C.A. Szigyarto, A. Persson, J. Ottosson, H. Wernerus, P. Nilsson, E. Lundberg, A. Sivertsson, S. Navani, K. Wester, C. Kampf, S. Hober, F. Ponten, M. Uhlen, A genecentric Human Protein Atlas for expression profiles based on antibodies, Mol Cell Proteomics, 7 (2008) 2019-2027.

[41] H. Slaastad, W. Wu, L. Goullart, V. Kanderova, G. Tjonnfjord, J. Stuchly, T. Kalina, A. Holm, F. Lund-Johansen, Multiplexed immuno-precipitation with 1725 commercially available antibodies to cellular proteins, Proteomics, 11 (2011) 4578-4582.

국문 초록

ROS1 은 타이로신 카이네이즈 수용체로, 유전자는 염색체 6 번에 위치하며 세포 내부의 타이로신 카이네이즈 도메인, 트랜스 멤브레인 그리고 세포 외부 도메인으로 구성이 되는 약 265 kDa 정도의 크기의 단백질이다. ROS 단백질은 염색체내의 빈번한 유전자 재배열 때문에 3'의 ROS1 과 5'의 파트너 단백질의 재조합 형태로 발현된다. 이러한 재조합 ROS1 단백질들을 이용한 연구는 꾸준히 수행되어 왔지만, 야생형 ROS1 에 대해서는 현재까지 보고된 바가 많이 없다. 더구나 ROS1 수용체는 알려진 라이간드가 없어 전체 길이의 야생형 ROS1 과 관련된 특징 및 기능에 대한 연구도 부족하다. 현재, 전체 길이의 야생형 ROS1 의 발현은 후성 유전학에 의해 조절이 된다는 가능성만이 제기되고 있는 실정이며, 그렇기 때문에 야생형 ROS1 을 발현하는 세포주를 개발하고, ROS1 의 N 말단에 결합하는 양질의 항체를 개발하고자 하는 필요성이 대두되었다. 이러한 전체 길이의 야생형 ROS1 의 검출과 연구를 위하여는 ROS1 의 N 말단 영역에 특이적으로 결합하는 항체가 필요하고, 본 연구를 통하여 마침내 N 말단에 특이적으로 항원반응성을 지닌 3B20 단일 사슬 항체가 개발되었다. 그러나 개발된 항체의 특성 분석을 수행하던 중, 항원 특이성의 시험법인 면역블롯(immunoblot) 과 면역침강반응(immune−precipitation) 분석에서 열충격단백질(Hsp)70 패밀리에 대한 교차 반응성이 있음이 확인되었다. 또한 전체길이의 야생형 ROS1 이 과발현된 세포주에 대한 면역침강반

응(Immunoprecipitation)과 질량분석(Mass spectrometry)의 실험 결과 아스파르트산, 류신, 글라이신, 그리고 트레오닌(DLGT)의 아미노산을 ROS1 과 Hsp70 패밀리가 공유하고 있음이 추가로 확인되었다. 개발된 3B20 단일 사슬 항체의 항원인식부분인 항원 결정 부위를 알아보기 위한 실험으로는 알라닌 스캐닝 돌연변이 유발(Alanine scanning mutagenesis)법이 수행되었고, 항체의 에피톱이 이 DLGT 아미노산을 포함하고 있음이 증명되었다. 이렇게 3B20 단일 사슬 항체의 특성을 분석하던 중 밝혀진 항체의 교차 반응성은 3B20 단일 사슬 항체의 중쇄 상보성 결정 영역 3 에 무작위 돌연변이를 도입하여 해결하고자 하였다. 결과적으로, 포인트 돌연변이가 도입된 새로운 3B20-H1-13 단일 사슬 항체는 특이적으로 ROS1 에는 결합하나, Hsp70 패밀리의 일종인 GRP75 에는 결합하지 않는다는 것이 효소면역측정법(ELISA) 및 면역블롯, 면역침강반응 실험을 통해 증명되었다. 최종적으로는 변형된 3B20-H1-13 단일 사슬 항체를 이용하여 전체 길이의 야생형 ROS1 의 발현 여부를 조사하고자 하였고, 면역 조직 화학적 분석 (IHC)에서 ROS1 은 종양이 아닌 폐 조직에서는 발견되지 않고 폐 선암에서 특이적으로 과발현되어 있음을 확인하였다. 본 연구는 야생형 ROS1 의 N 말단에 결합하는 단일 사실 항체의 개발과 개발 후 생산 및 특이성 증대에 대하여 서술되었다. 선별된 항 ROS1 항체인 3B20 단일 사슬 클론은 Hsp70 패밀리에 교차 반응성을 지니고 있었지만 중쇄 상보성 결정 영역 3 (HCDR 3)에 무작위 돌연변이 유발을 사용하여 항체의 반응

특이성이 개선되었다. 이러한 3B20 단일 사슬 항체의 특이성은 최종적으로 ROS1 에 대한 결합 친화도를 유지하면서 교차 반응성은 감소되도록 유도되었다. 본 연구에서 개발된 ROS1 의 N 말단에 특이적으로 결합하는 항체를 이용하면 야생형 ROS1 에 대한 발현 및 기능 연구에 많은 도움이 될 것으로 기대되는 바이다.

주요어

ROS1, 야생형 ROS1, 항원 반응 특이성, 돌연변이, 단일 사슬 항체

학 번

2009-21902

본 학위 논문의 결과는 *Biochemical and Biophysical Research Communications 2017 Nov 4;493(1):325-331* 에 출간 되었습니다.